Geological and geomorphological evolution of a sedimentary periglacial landscape in Northeast Siberia during the Late Quaternary

Guido Grosse [a,*], Lutz Schirrmeister [a], Christine Siegert [a], Viktor V. Kunitsky [b], Elena A. Slagoda [c], Andrei A. Andreev [a], Alexander Y. Dereviagyn [d]

[a] *Alfred Wegener Institute for Polar and Marine Research, Research Unit Potsdam, Telegrafenberg A43, 14473 Potsdam, Germany*
[b] *Permafrost Institute, Russian Academy of Science, Yakutsk, Merzlotnaya Street, Yakutsk, 677010 Russia*
[c] *Institute of Earth Cryosphere, Russian Academy of Sciences, Malygin Street 86, Tyumen, 625026 Russia*
[d] *MGU Moscow State University, Faculty of Geology, Russia, Vorobievy Gory, 119899 Moscow, Russia*

Abstract

A wide variety of environmental records is necessary for analysing and understanding the complex Late Quaternary dynamics of permafrost-dominated Arctic landscapes. A NE Siberian periglacial key region was studied in detail using sediment records, remote sensing data, and terrain modelling, all incorporated in a geographical information system (GIS). The study area consists of the Bykovsky Peninsula and the adjacent Khorogor Valley in the Kharaulakh Ridge situated a few kilometres southeast of the Lena Delta. In this study a comprehensive cryolithological database containing information from 176 sites was compiled. The information from these sites is based on the review of previously published borehole data, outcrop profiles, surface samples, and our own field data. These archives cover depositional records of three periods: from Pliocene to Early Pleistocene, the Late Pleistocene and the Holocene. The main sediment sequences on the Bykovsky Peninsula consist of up to 50 m thick ice-rich permafrost deposits (Ice Complex) that were accumulated during the Late Pleistocene. They were formed as a result of nival processes around extensive snowfields in the Kharaulakh Ridge, slope processes in these mountains (such as in the Khorogor Valley), and alluvial/proluvial sedimentation in a flat accumulation plain dominated by polygonal tundra in the mountain foreland (Bykovsky Peninsula). During the early to middle Holocene warming, a general landscape transformation occurred from an extensive Late Pleistocene accumulation plain to a strongly thermokarst-dominated relief dissected by numerous depressions. Thermokarst subsidence had an enormous influence on the periglacial hydrological patterns, the sediment deposition, and on the composition and distribution of habitats. Climate deterioration, lake drainage, and talik refreezing occurred during the middle to late Holocene. The investigated region was reached by the post-glacial sea level rise during the middle Holocene, triggering thermo-abrasion of ice-rich coasts and the marine inundation of thermokarst depressions.
© 2006 Elsevier B.V. All rights reserved.

Keywords: Quaternary environment; Periglacial landscape; Permafrost; Thermokarst; Remote sensing; GIS

1. Introduction

Since permafrost deposits and periglacial geomorphology in NE Arctic Siberia are excellent indicators of landscape and environmental dynamics, they have been

* Corresponding author. Present address: Geophysical Institute, University of Alaska Fairbanks, 903 Koyukuk Drive, P.O. Box 757320 Fairbanks, AK 99775-7320, USA.
  E-mail address: ggrosse@gi.alaska.edu (G. Grosse).

a major research topic in Late Quaternary palaeo-environmental reconstruction for many years. During the Late Pleistocene, the global sea level was lowered by about 120 m (Fairbanks, 1989). The shallow shelves of the Laptev, East Siberian, and Chukchi Seas in NE Siberia that are several hundred kilometres wide were subaerially exposed, being part of the Beringia Land. There is no analogue in the present landscapes of the northern hemisphere. Due to a strongly continental climate, the Northeast Siberian shelf regions were not covered by an ice sheet at least since the Late Saalian (Hubberten et al., 2004; Svendsen et al., 2004). Indications for embryonal glaciation in limited areas are evident, e.g. in the presence of large nival cirques in the coastal mountain ranges (Galabala, 1997). Large parts of the flat shelf regions were characterised by the deposition of fine-grained ice- and organic-rich sediments of the so-called Ice Complex (IC) and of fluvial sediments in major river valleys during the Late Pleistocene cooling period.

During the post-glacial marine transgression and the beginning of the Holocene warming, shelf submergence and thermokarst development destroyed most parts of this depositional environment (Romanovskii et al., 2004). Today, the IC still covers large areas in the Northeast Siberian coastal lowlands and on islands in the Laptev and East Siberian Seas, which are subject to continuing coastal erosion (Gavrilov et al., 2003).

The Ice Complex is a syncryogenic deposit of fine-grained sediments with segregated ice and syngenetic ice wedges resulting in volumetric ice contents up to 80–90%. The IC contains rich palaeo-environmental information preserved in the sediments, ground ice, and frozen fossil remains. A wide variety of environmental proxies were used for the reconstruction of the Late Quaternary environment of the Laptev Sea region, such as pollen (Andreev et al., 2002), ground ice (Meyer et al., 2002a,b), sediments (Schirrmeister et al., 2002a), testate amoebae (Bobrov et al., 2004), plant macro fossils (Kienast et al., 2005), and insect and mammal remains (Sher et al., 2005). Many hypotheses about the IC origin have been debated in the last decades. In these hypotheses, assumptions about the origin and regional genesis of the IC were often based only on sparse, local and site-specific data. Moreover, the context of environmental dynamics (i.e. sediment sources, transport areas, and accumulation areas) in an entire landscape was rarely considered. Sher et al. (2005) favour the hypothesis of a polygenetic origin, more reflecting a certain climatic situation rather than a particular depositional agent. The IC was formed under a generally very cold and highly continental climate, with intense cryogenic weathering and other permafrost processes and phenomena. According to Sher et al. (2005), this resulted in a similar appearance of deposits although they formed in various environments and under different depositional regimes like fluvial, aeolian, lacustrine, or proluvial.

One of the most researched Ice Complex locations in Siberia is the Mamontovy Khayata outcrop at the eastern coast of the Bykovsky Peninsula, 20 km south-east of the Lena Delta (Fig. 1A,B). A large number of radiocarbon dates (Schirrmeister et al., 2002b) allow detailed palaeo-environmental reconstructions at the key site of Mamontovy Khayata, but also for the regional depositional history, landscape evolution, and IC origin.

In this paper we demonstrate the combination of a wide variety of data from different sources to reconstruct the periglacial landscape evolution in this region during the Late Quaternary. We constructed a comprehensive database containing all available cryolithological and stratigraphical field information. Data from this database was then analysed along with terrain and remote sensing data using a geographical information systems (GIS) approach. This approach allowed the creation of a landscape evolution scheme and the examination of the genetic relationship between the Bykovsky Peninsula permafrost sequences and the mountainous hinterland including the Khorogor Valley.

In contrast to the existing palaeo-environmental reconstructions of individual outcrop sections or boreholes, our landscape dynamics approach resulted in a more comprehensive understanding of the palaeo-environmental conditions, especially in terms of spatial and temporal variability. The derived general concept of landscape evolution is applicable to many regions in the Laptev Sea coastal lowlands, where similar geomorphological settings including low mountain ranges and an adjacent IC accumulation plain are widely distributed.

2. Regional setting

The Bykovsky Peninsula and the adjacent Khorogor Valley are located on the northern margin of the Siberian mainland at the Laptev Sea coast (Fig. 1A,B). The region is dominated by arctic tundra, a strongly continental climate, and periglacial processes (Treshnikov, 1985). The continuous permafrost in the region has temperatures of −9 °C to −11 °C and reaches down to 300–500 m depth below the surface (Yershov, 1998). The region consists of two main geological parts (Fig. 1B). In the east, the Kharaulakh Ridge with heights up to 500 m a.s.l. represents the northern foothills of the Verkhoyansk
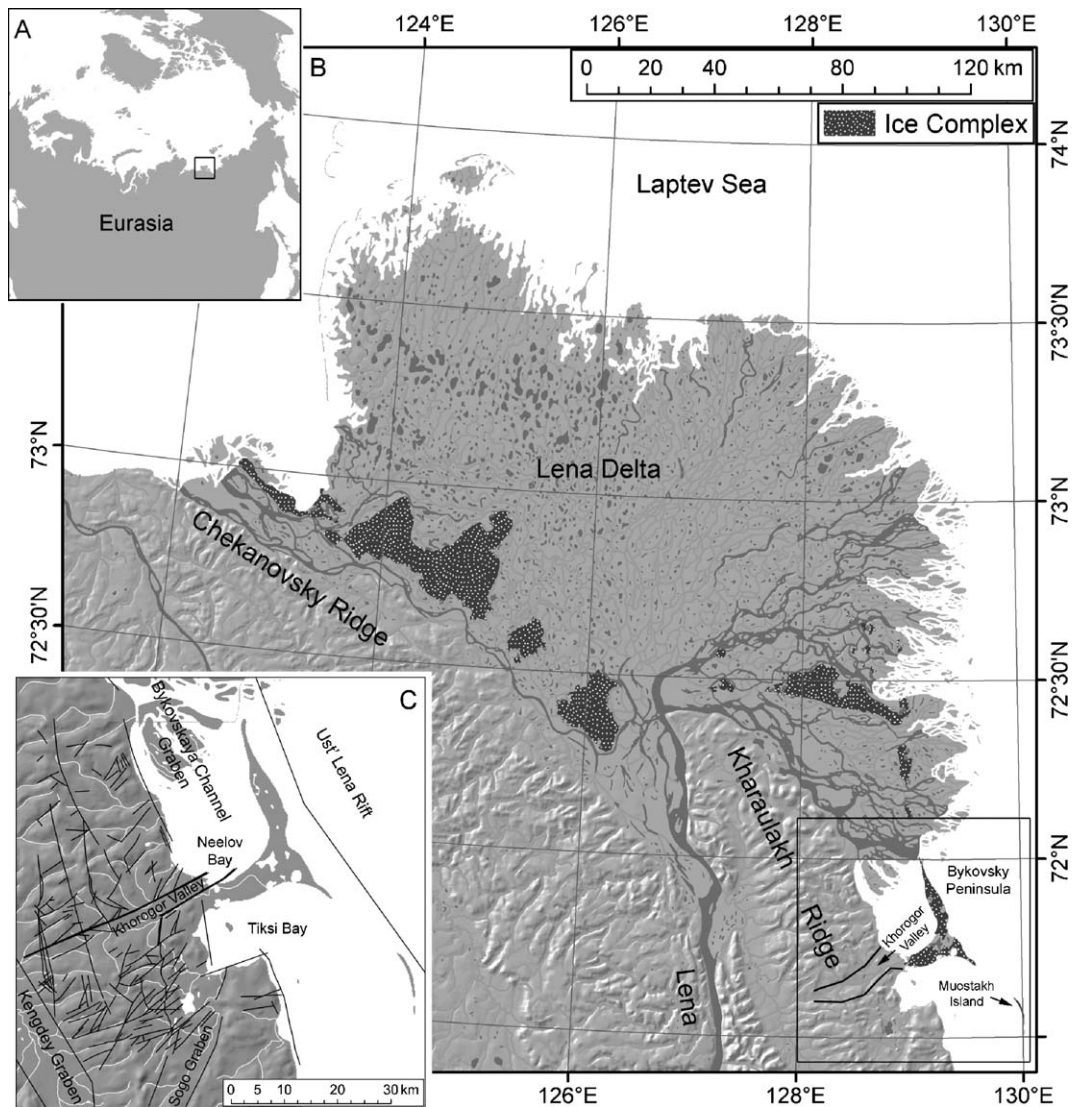
Fig. 1. The study area. A) Location of the study area in NE Siberia (black box). B) Shaded relief map showing the location of the Bykovsky Peninsula and the Khorogor Valley in the SE of the Lena Delta (black box). The modern distribution of erosional remnants of Ice Complex deposits in the Lena Delta region was derived by geomorphological mapping with Landsat-7 ETM+images and field data. C) Subset of the investigated region showing the location of tectonical faults and lineaments according to previous studies (Grigoriev et al., 1996; Drachev et al., 1998; Ursov et al., 1999; Imaev et al., 2000; Parfenov, 2001). Note the two major faults (thick black lines) along the Khorogor Valley boundary.

Mountains. Farther east, the Bykovsky Peninsula represents the remains of a former accumulation plain with elevations of up to 45 m a.s.l. The stratigraphic map of Sergienko et al. (2004) distinguishes two structural regions: the so-called "Kharaulakhsky Rayon" (including the Khorogor Valley) with a general uplift tendency during the Pleistocene and Holocene, and the "Buor-khainsky Rayon" (including the Bykovsky Peninsula) with a general subsidence tendency.

The Kharaulakh Ridge consists mainly of permo-carboniferous sandstones and slates, which are characterised by strong dissection due to tectonic activity during

the Cenozoic. Neotectonic activity in the wider region is proven by seismic studies (Grigoriev et al., 1996; Drachev et al., 1998; Imaev et al., 2000; Franke et al., 2001). The Khorogor Valley is the largest of several SW–NE orientated valleys within dislocation zones in the northern Verkhoyansk Mountains. It is 30 km long and about 10 km wide at the mouth. The valley shape is probably strongly influenced by tectonics. Imaev et al. (2000) indicate two major WSW–ENE striking faults along the valley flanks (Fig. 1C). Along these two lineaments the Khatys-Yuryakh and Khorogor Rivers flow towards the Neelov Bay in a NE direction. According to Grinenko and

Imaev (1989), the Neelov Bay shore at the valley mouth is formed by a major SSE–NNW striking fault bordering the Bykovsky Channel Graben. No traces of extensive glaciations were found in the low-lying Kharaulakh Ridge, although glaciers occurred in the higher Verkhoyansk Mountains to the south during the Late Pleistocene (e.g. Kind, 1975). Thus, periglacial and nival processes were the most important factors for weathering, erosion, transport, and accumulation in the Kharaulakh Ridge.

The Bykovsky Peninsula, situated to the east of the Khorogor Valley, consists of uplands of ice-rich permafrost, and deep depressions and valleys formed by thermokarst and thermo-erosion. The uplands, called Yedoma, mostly consist of ice-rich, fine- to medium-grained sandy permafrost deposits of the Late Pleistocene IC. The ground ice occurs in the form of large ice wedges of up to 5 m in width and up to 40–50 m in depth, and segregated ice in the form of subhorizontal ice bands and small ice lenses. The deposits are often very organic-rich and contain palaeosols and peat horizons. The depressions and valleys contain a variety of reworked IC sediments (slope deposits) or newly formed deposits (i.e. peat and lacustrine sediments). The transgression of the Laptev Sea after the Last Glacial Maximum (LGM) reached the area of the Bykovsky region during the middle–late Holocene (Bauch et al., 2001). The Bykovsky Peninsula and a few other similar, but smaller erosional remnants in the south (Muostakh Island) and north (several islands in the eastern Lena

Delta consisting of IC; Fig. 1) were part of an extended accumulation plain. During the Late Pleistocene, this plain probably covered large parts of the flat subaerial Laptev shelf in front of the low mountain ranges. The modern shore of the peninsula is continuously shaped by thermo-abrasion and other coastal processes.

3. Data and methods

We used various data sources for our analysis and reconstruction of the regional landscape development during the Late Quaternary (Fig. 2). We integrated the currently available information from a cryolithological field database, remote sensing imagery, geomorphological mapping, and a digital elevation model (DEM) in a GIS software package (ArcGIS™).

3.1. Cryolithological field database

Our database contains currently available information on sedimentology and cryolithology for the investigation area. This information was acquired from boreholes, outcrop sections, subsurface samples and surface samples. Most previous investigators focussed on data sampling from coastal sections and core drilling in the Bykovsky Peninsula. We additionally investigated several new sites in the adjacent Khorogor Valley. Thus, the data in the database originates from our own field work, previous publications, published and unpublished field reports, and personal communications (Kunitsky,
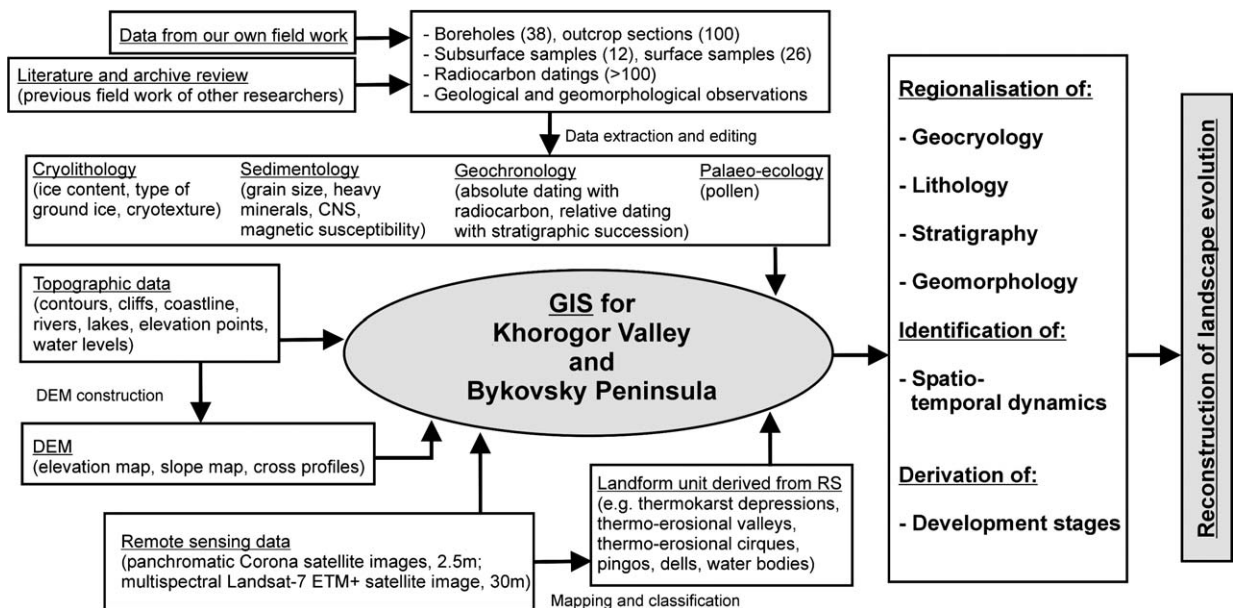

Fig. 2. Flowchart of the study concept.

1989; Slagoda, 1993; Grigoriev, 1993; Grigoriev et al., 1996; Siegert et al., 1999; Sher et al., 2000; Schirrmeister et al., 2001; Siegert et al., 2002; Schirrmeister et al., 2002a,b; Grosse et al., 2003; Kholodov et al., 2003; Sher et al., 2005; Kholodov, pers. comm.). Obviously, the quality of the data is heterogeneous. For some older data, no original descriptive material was available, thus the information was extracted from schematically drawn drill logs or outcrop profiles. For some sites, only poor descriptions of location and/or geocryology were available. We only used data with reliable records of geocryological conditions and accurate site locations. In total, data for 176 sites were compiled in the database and loaded into the GIS (Fig. 3). The database contains information on location, type of data acquisition, date of fieldwork, primary investigator, data reference, and identified cryolithological layers. For each layer,

lithology, geocryology, fossil remains, interpreted facies and stratigraphy, and existing dates were recorded. General geological and geomorphological field observations were also added for supporting the upscaling of information from local to regional.

The geochronology of the investigation area is based on more than 100 radiocarbon dates (Fig. 4). Most of the dates were acquired in the Mamontovy Khayata outcrop section (Tomirdiaro et al., 1984; Kunitsky, 1989; Slagoda, 1993; Nagaoka, 1994; Nagaoka et al., 1995; Schirrmeister et al., 2002b; Slagoda, 2004). Seventy-six radiocarbon dates were published by Schirrmeister et al. (2002b) for Mamontovy Khayata and some adjacent thermokarst structures. Other sites on the Bykovsky Peninsula were dated by Slagoda (1993) (Table 1). Additionally, we present 23 new radiocarbon dates from the region including the first AMS dates from the
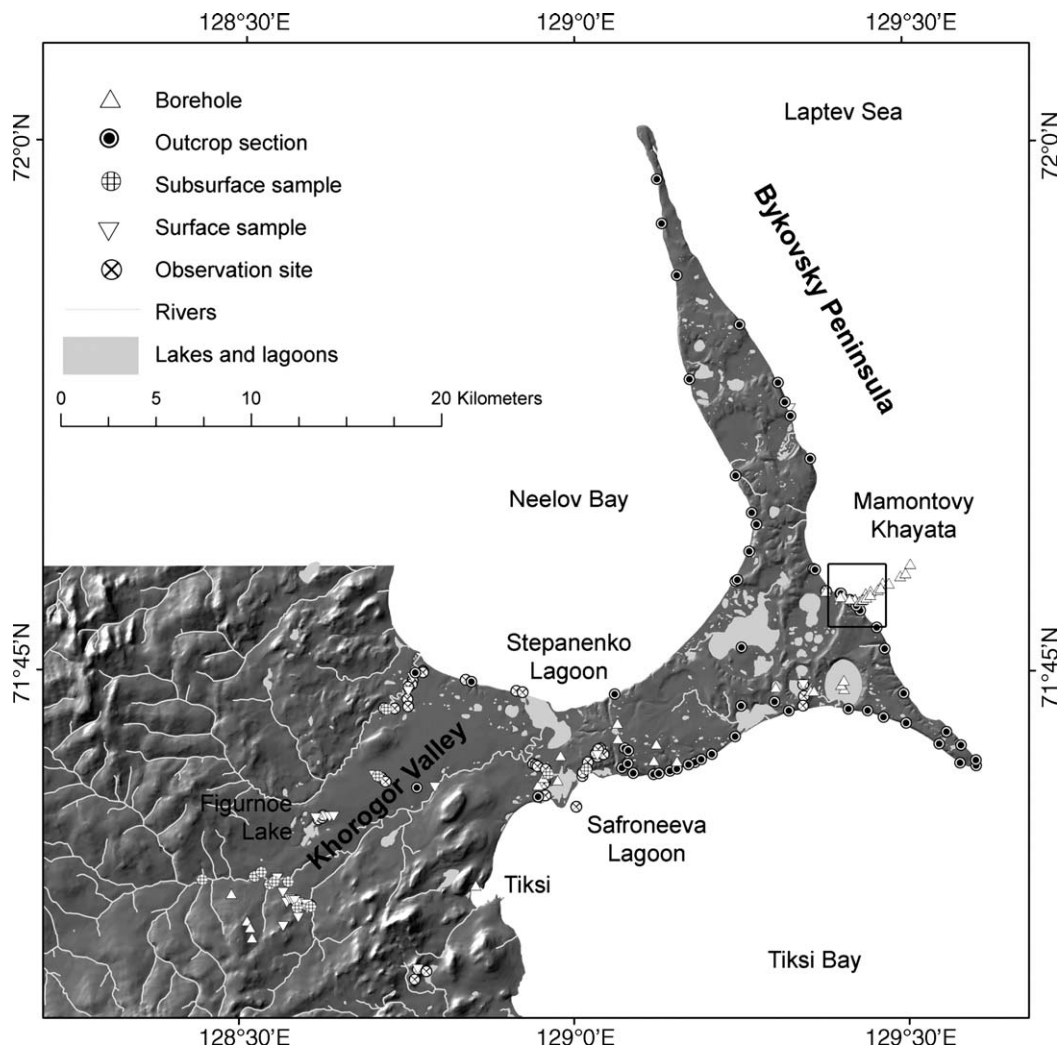

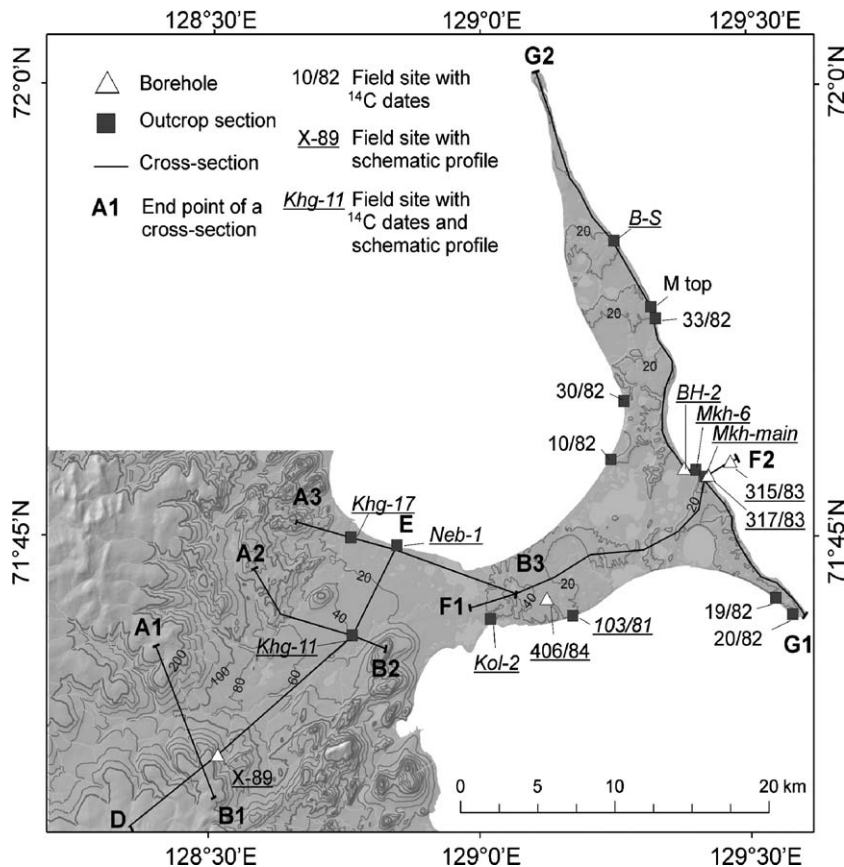Fig. 3. Shaded relief map with the locations of 176 field sites.

Fig. 4. Topographic map showing the locations of schematic profiles (Figs. 6–8), sites with ^{14}C dates (Table 1), and geomorphological cross-sections (Fig. 5).

Khorogor Valley (Table 1). Pollen diagrams and palaeo-ecological interpretations are also presented for these new records from the Khorogor Valley.

3.2. Remote sensing imagery

Optical remote sensing was used as a tool for identifying morphological land surface features, analysing their spatial distribution, detecting landscape forming processes, and upscaling cryolithological information. Two panchromatic CORONA satellite images taken on 24th July 1969 with 2.5 m ground resolution were used for mapping periglacial surface features (Grosse et al., 2005). The images were digitised, digitally enhanced, geo-referenced, and finally mosaiced. Mapped surface features in the study area include thermokarst depressions, thermo-erosional valleys, thermo-erosional cirques, thermokarst lakes, thermokarst lagoons, thermokarst mounds, and pingos. Additional features investigated in the Khorogor Valley include cryoplanation terraces, slope wash areas, small rivers, small

thermokarst lakes, thermokarst mounds, and ice wedge polygons.

To enhance feature identification, the high-resolution CORONA images were combined with a DEM or with multispectral Landsat-7 ETM+ data, respectively, based on the overlay of both image types as semi-transparent GIS-layers. The Landsat-7 data with 30 m ground resolution (e.g. Goward et al., 2001) were especially helpful for the discrimination of geomorphological structures dominated by different vegetation complexes. We used the Landsat-7 band combinations of 3-2-1 (true colour) and 5-4-3 (short-wave infrared–near infrared — red), as these provided the highest contrasts among geomorphological structures.

Periglacial surface structures can be related to various relief forming processes. Some structures indicate permafrost degradation (e.g. thermo-erosional valleys, thermokarst lakes, and thermokarst hills), other permafrost aggradation (e.g. Yedoma uplands, pingos, and ice wedge polygons in drained basins). The nesting or coexistence of such structures is common in

Table 1
Radiocarbon dates from various sites in the Khorogor Valley and the Bykovsky Peninsula

Outcrop or sample no.	Lab code[a]	Deposit type	Dated material	Altitude m a.s.l.	Radiocarbon age y BP	y cal BP (2 sigma)[b]	Source
Khorogor Valley							
Khg-11/1	KIA 25714	Valley bottom, IC	Peat	36	11 545±45	13 552–13 308	This work
Khg-11/2	KIA 20692	Valley bottom, IC	Peat	35.4	11 710±50	13 886–13 450	This work
Khg-11/3	KIA 20693	Valley bottom, IC	Peat	35	12 145±55	14 365–14 036	This work
Neb-1/11	KIA 20699	Alluvial	Peat	4.5	945±25	873–816	This work
Neb-1/10	KIA 25713	Alluvial, IC	Twigs	4.2	10 440±40	12 695–12 080	This work
Neb-1/6	KIA 20698	Alluvial, IC	Peat	3.45	10 690±55	12 964–12 617	This work
Neb-1/2	KIA 20697	Alluvial, IC	Peat	2.6	11 260±40	13 455–13 016	This work
Neb-1/1	KIA 20696	Alluvial, IC	Plant remains	2.1	11 400±100	13 513–13 139	This work
Khg-17/12	KIA 20695	Valley bottom, IC	Peat	7	10 120±50	12 115–11 546	This work
Khg-17/7	KIA 25712	Valley bottom, IC	Twigs	6	10 210±55	12 336–11 641	This work
Khg-17/1	KIA 20694	Valley bottom, IC	Peat	4.8	10 190±70	12 330–11 553	This work
Bykovsky Peninsula, Holocene deposits							
Kol-2/2	KIA 20701	Holocene cover on IC	Peat	14.0	4555±30	5320–5256	This work
Kol-2/1	KIA 20700	Holocene cover on IC	Peat	13.8	4720±35	5411–5326	This work
MKh-4.6-2	KI 4856	Holocene cover on IC	Peat	36.65	7310±65	8213–7973	This work
19/82	IM-764	Holocene cover on IC	Peat	22.0	4430±300	5755–4241	Slagoda (1993)
20/82	IM-765	Holocene cover on IC	Peat	21.5	5450±150	6564–5918	Slagoda (1993)
10/82	IM-763	Alas deposit	Wood	11.0	9450±100	11 116–10 488	Slagoda (1993)
33/82	IM-762	Alas deposit	Wood	8	9250±500	12 059–9248	Slagoda (1993)
Bykovsky Peninsula, Pre-Holocene deposits							
MKh02-1/1	KIA 25715	IC, top	Twigs	36.35	10 620±45	12 931–12 607	This work
MKh02-1/3	KIA 25716	IC, top	Twigs	35.25	12 890±50	15 912–14 485	This work
MKh02-1/5	KIA 25717	IC, top	Twigs	34.75	14 760±60	18 212–17 161	This work
B-S-2b	KIA 8167	Fluvial sand	Wood	22.0	13 410±55	16 591–15 666	This work
B-S-5	KIA 8166	IC	Wood	20.0	19 330±100	23 321–22 555	This work
B-S-7	KIA 8165	IC	Peat	10.0	53 020+2670/−2000		This work
Byk-BH-2-21	KIA 11443	Fluvial sands in a pingo	Twigs, l.r h.a.	22.3	>53 000 30 950+690/−640		This work
MKh-6.3−1	KIA 6737	IC, taberite	Grass roots	2.0	47 400+2730/−2030		This work
M-1.2	KIA 8164	IC	Twigs	24	35 050+340/−330		This work
30/82	IM-767	IC	Peat	20.0	28 180±300		Slagoda (1993)
19/82	IM-766	IC	Peat	11.0	23 700±500		Slagoda (1993)
103/81	LU-1328	IC	Peat	7.0	21 630±240		Slagoda (1993)
103/81	LU-1130	IC	Peat	6.0	33 040±810		Slagoda (1993)
103/81	GIN-4597	IC	Plant material	5.0	40 200±1200		Slagoda (1993)
103/81	GIN-4593	IC	Plant material	4.0	40 400±1200		Slagoda (1993)
103/81	GIN-4391	IC	Plant material	2.5	40 800±1600		Slagoda (1993)

Site locations are shown in Fig. 4.

[a] Sample code KIA indicates AMS radiocarbon datings carried out at the Leibniz Laboratory for Radiometric Dating and Stable Isotope Research, Kiel University (Germany); All others are conventional radiocarbon dates from various Russian facilities.

[b] Calibration was done using CALIB 4.3; 5.0 (Stuiver et al., 1998).

periglacial landscapes like those in the Bykovsky Peninsula. Information about the spatial relations and temporal successions of surface structures and processes can be used for establishing a relative geochronology for the entire landscape. Subsequently, the identified surface structures were related to different landscape development stages by extrapolating the available cryolithological and geochronological information.

3.3. Terrain data

Several 1:100 000 topographic maps of the investigation area were acquired and subsequently scanned, geo-referenced and manually digitised. Using the map height information, a 30 m resolution DEM was produced for the investigation area by applying the TOPOGRID tool of ArcInfo™ (Fig. 4). The applicability
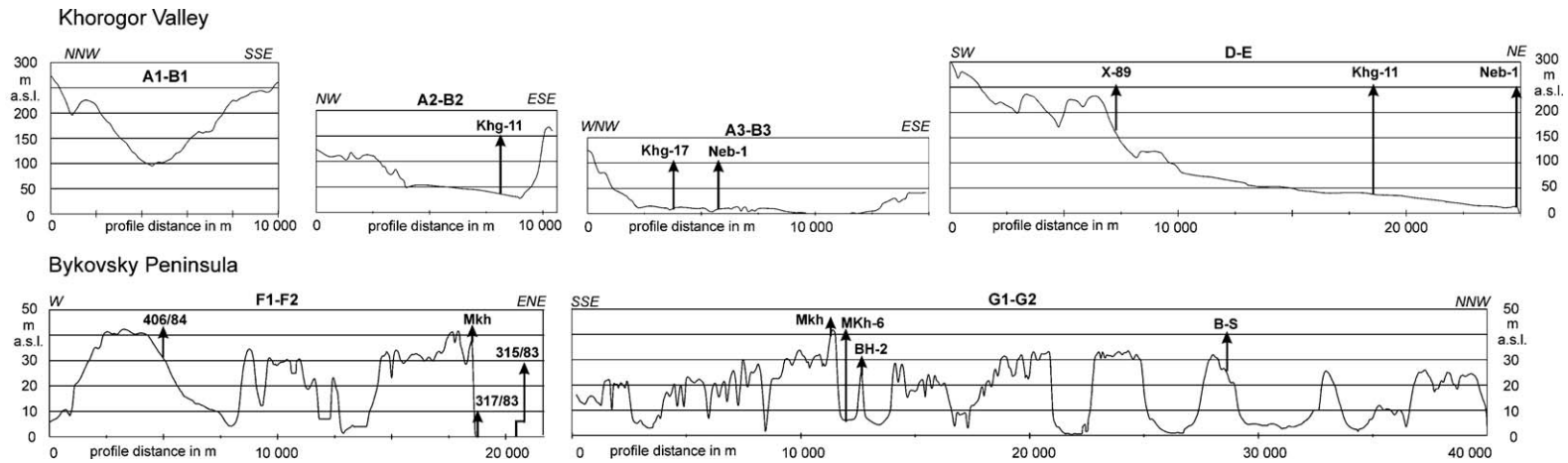
ARTICLE IN PRESS

Fig. 5. Topographic cross-sections. Upper: Khorogor Valley (A1–B1: upper valley; A2–B2: central valley, A3–B3: lower valley; D–E: transect along the valley axis; vertical exxageration 22:1). Lower: Bykovsky Peninsula (F1–F2: east–west transect; G1–G2: south–north transect along the east coast; vertical exxageration 110:1). Locations of the cross-sections are shown in Fig. 4. Arrows indicate the locations of the profiles shown in Figs. 6–8.

of this process chain for producing a reliable DEM of thermokarst-affected periglacial lowlands is demonstrated by Grosse et al. (2006). Then various DEM derivates were obtained including slope maps, shaded relief maps, and cross-sections for the Khorogor Valley and the Bykovsky Peninsula (Fig. 5).

4. Results

4.1. Sediment studies

We selected representative geological profiles providing key information for developing our landscape evolution scheme (Table 2). The sedimentary sequences in the investigation area include the Pliocene to Early Pleistocene deposits at the base, followed by Late Pleistocene deposits of the Early Weichselian Glacial (Zyryan), the Middle Weichselian Interstadial (Karginsky), the Late Weichselian Glacial (Sartan), and the Holocene according to the East Siberian Quaternary

Table 2
Key geological profiles used for reconstructing landscape evolution

Key profile	Profile type	Location	Source	Figures
X-89	Borehole	Upper Khorogor Valley	Slagoda (1993)	Figs. 4 and 6
Khg-11	Outcrop section	Central Khorogor Valley	This paper	Figs. 4 and 6
Khg-17	Outcrop section	Lower Khorogor Valley	This paper	Figs. 4 and 6
Neb-1	Outcrop section	Lower Khorogor Valley	This paper	Figs. 4 and 6
406/84	Borehole	Western Bykovsky Peninsula	Kunitsky (1989)	Figs. 4 and 7
103/81, 203/82	Combined profile of 2 outcrop sections	Western Bykovsky Peninsula	Slagoda (1993)	Figs. 4 and 7
Kol-2	Outcrop profile	Western Bykovsky Peninsula	This paper	Figs. 4 and 7
Mamontovy Khayata, MKh-6, 315/83, 317/83	Combined profile of several outcrop sections and 2 boreholes	Eastern Bykovsky Peninsula	Schirrmeister et al. (2002a), Kunitsky (1989)	Figs. 4 and 8
BH-2	Borehole	Eastern Bykovsky Peninsula	This paper	Figs. 4 and 8
B-S	Outcrop section	Eastern Bykovsky Peninsula	This paper	Figs. 4 and 8

Stratigraphy (Stratigrafiya SSSR, 1982, 1984; Velichko, 1999). These Late Quaternary periods correspond to MIS 4 to 1, respectively.

4.1.1. Khorogor Valley

Borehole X-89, located at 160 m a.s.l., proved the presence of at least 30 m thick sediments on some slopes in the upper valley regions (Figs. 4 and 6). Above the bedrock, a thin layer of cryogenic eluvium occurs, which is interpreted as Pliocene to Early Pleistocene by Slagoda (1993). Following is a 15 m sequence of ice-poor pebbles in a silty–sandy matrix, interpreted as Early Pleistocene alluvial deposits. The next 12 m above consist of fine-grained silty–sandy sediments interbedded with some gravel. This horizon has a high ice content (30–90%) and contains plant remains, which are partially *in situ* (grass roots), and is interpreted as Late Pleistocene proluvial IC deposits. The upper 2 m, interpreted as Holocene sediments, consist of peat with silty–sandy interlayers. The sequence in X-89 has been verified by additional borehole records from nearby valley slopes (Slagoda, 2005). In contrast to the thick sediments there, further northeast the bottom of the upper valley around Figurnoe Lake (Fig. 3) is only covered by coarse-grained weathering debris and a thin peat layer above bedrock.

Outcrop Khg-11 was in a thermokarst mound, which has formed at 36 m a.s.l. on the bottom of the central valley (Figs. 4 and 6). Above weathered slate at the base, two 10 cm layers of alluvial gravel and silty sand were found and interpreted as deposits of the Sartan Glacial. These are followed by a 1.1 m thick peat horizon dated with three radiocarbon samples to the Bølling/Allerød (Table 1). The peat is covered by a 10 cm alluvial layer of silty sand. The spacing between thermokarst mounds suggests the former presence of wide ice wedges between them.

The lower 2.2 m of outcrop Neb-1 on the shallow cliff of the Neelov Bay shore consist of fine-grained sandy alluvial deposits with small pebbles (Figs. 4 and 6). The deposits have a massive cryostructure with large ice wedges and some ice bands. Four peat inclusions were dated to the Bølling/Allerød and the Younger Dryas (Table 1). Above the alluvial deposits a 0.7 m thick peat horizon is located, dated with a subrecent age.

Outcrop Khg-17 is a thermokarst mound, located on the eastern bank of the Khatys-Yuryakh River (Fig. 4) close to the river mouth (4.5–7.5 m a.s.l.). The lower 2.5 m consist of alluvial silty–sandy sediments with peat inclusions but without visible cryostructure (Fig. 6). Three radiocarbon dates from the lower and the upper part of this horizon are dated to the Late Glacial/Holocene transition (Table 1).
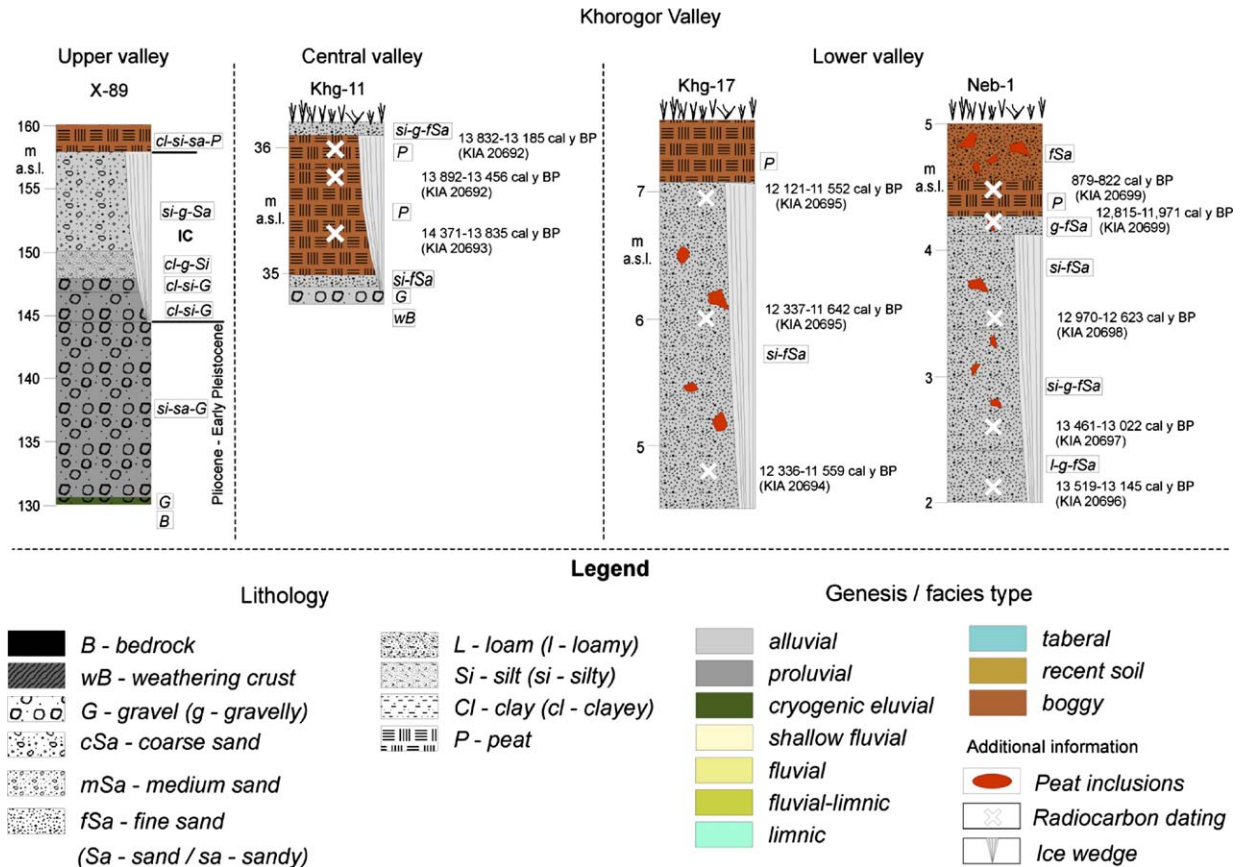
Fig. 6. Schematic sedimentological profiles for outcrops in the Khorogor Valley: borehole X-89 from a slope in the upper valley (Slagoda, 1993), section Khg-11 from a thermokarst mound in the central valley, section Khg-17 from a river bank in the lower valley, and section Neb-1 from a cliff on the Neelov Bay shore. For profile locations see Fig. 4.

To summarise, the bottom of the lower and middle valley up to 36 m a.s.l. is covered by late Sartanian deposits. Thermokarst mounds several metres high prove the existence of at least several metre thick sediments and thick ice wedges at some locations. These deposits should be interpreted as the remains of IC formed at the very end of the Pleistocene.

4.1.2. Western Bykovsky Peninsula

Borehole 406/84 (Fig. 4) covers sediment sequences from 25 m b.s.l to 32.5 m a.s.l. (Fig. 7). The lowest 25 m are fluvial coarse-grained sandy and gravelly deposits with plant remains and a massive cryostructure. The deposits are interpreted as taberal Early Quaternary sediments (Grigoriev, 1993). Taberal deposits are permafrost sediments that underwent thawing in a talik and subsequent refreezing from all sides (Konishchev et al., 1999), resulting in special sedimentary structures, cryotextures, and often depleted organic carbon. They are followed by 5 m of alluvial interbeddings of silty–sands, gravels, and silts with banded cryostructure (Zyryan IC).

This sequence is followed by 27 m of proluvial, silty–sandy IC deposits (Karginsky and Sartan deposits). They are ice-rich and contain ice wedges, ice bands, and peat inclusions. The upper 0.5 m consists of an unfrozen Holocene soil.

Combined profile 103/81-203/82 is close to this borehole, thus the lithological composition is very similar (Fig. 7). Five dates exist between 2.5–7 m a.s.l., ranging from the Karginsky to the early Sartan (Slagoda, 1993; Table 1).

Outcrop Kol-2 is situated at 14–15 m a.s.l. in a small erosive brook that followed the ice wedge net on a Yedoma slope. The deposits consisted largely of peat, which was dated with two radiocarbon samples to the middle Holocene (Fig. 7, Table 1).

4.1.3. Eastern Bykovsky Peninsula

The Mamontovy Khayata section was studied multidisciplinary (e.g. Kunitsky, 1989; Slagoda, 1993; Schirrmeister et al., 2002a,b; Siegert et al., 2002; Andreev et al., 2002; Sher et al., 2005). Therefore, we
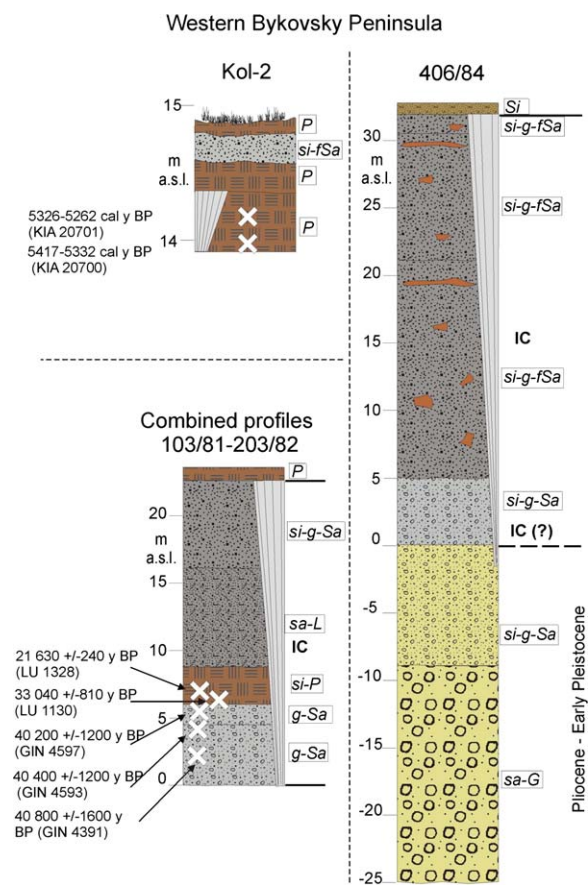
Fig. 7. Schematic sedimentological profiles for outcrops in the western part of the Bykovsky Peninsula: section Kol-2 from a gentle slope on the flank of an Ice Complex elevation; a combined profile of sections 103/81-203/82 from the southern coast at Cape Razhdelny (Slagoda, 1993); and borehole 406/84 from an IC Complex elevation in the hinterland of Cape Razhdelny (Kunitsky, 1989). For profile locations see Fig. 4. The legend is shown in Fig. 6.

give only a short description of the profile, combined with adjacent profiles from a thermokarst depression and two offshore boreholes. The covered sequence is 89 m thick, ranging from 51 m b.s.l. to 38 m a.s.l. (Fig. 8). From 51–9 m b.s.l. sandy to gravelly fluvial deposits are located, and they were interpreted as Pliocene–Early Pleistocene (Kunitsky, 1989). They are followed discordantly by shallow fluvial or more general alluvial fine-grained sandy deposits (9 m b.s.l.–8 m a.s.l.), which are considered as Zyryan IC containing typical lens-like reticulated cryostructure, ice bands, and ice wedges. *In situ* grass roots, small twigs and peat inclusions were frequently found. The age interpretation of this lowermost IC is guided by several dates of the upper parts exposed near the sea level, which are close to the radiocarbon dating limit. Extrapolated age estimations

for the IC were derived from an age–height relation based on uncalibrated radiocarbon ages and mean accumulation rates (Meyer et al., 2002a). They suggest the start of IC sedimentation at around 80 ky BP. The next IC horizon with silt, clayey silt and silty sand at 8–23 m a.s.l. is interpreted as Karginsky deposits. This ice-rich horizon contains many palaeosols and peat inclusions. From 23–36 m a.s.l. the IC consists of ice-rich silty to fine sand and is additionally characterised by lower organic carbon contents and the heaviest $\delta^{13}C$ values (Siegert et al., 2002), which are indicative of Sartan Ice Complex deposits. The following uppermost 2 m of peat-rich silts are dated of Holocene ages. A sedimentary gap exists on top of the IC of the Mamontovy Khayata main section between ca. 9.4 and 12.5 cal ky BP at the transition from the Sartan to the Holocene. The sedimentation rate was relatively stable during the Late Pleistocene, which is suggested by the clear age–height relation in the deposits. In addition, large syngenetic ice wedges of 5–6 m in width and 40 m in depth are embedded in the sediment, and segregated ice with syncryogenic patterns (ice bands and lens-like reticulated cryostructure) is common. The ground ice content of the IC rises up to 100–170% by weight.

The deposits in the adjacent thermokarst depression (MKh-6, Figs. 4 and 8) consist of silty to coarse-grained sandy sediments. They have formed under various conditions as fluvial–limnic or proluvial deposits. Below these thermokarst deposits taberal IC sediments occur. The dating of the thermokarst deposits shows early–late Holocene ages (Schirrmeister et al., 2002b; Table 1). The early Holocene deposits (ca. 11.5 ky cal BP) occur in terraces, which are formed on slopes of the depressions. The sediments of the thermokarst depression are far less ice-rich (30–60% by weight) than the IC, although the ice wedges are 3–4 m wide and several metres deep. The ground ice in the frozen sediment is distributed mainly in fine pores as massive cryostructure. The formation of some peat horizons indicates alternating stages of thermokarst subsidence and stagnation. Sedimentary structures like graded bedding and ripples occur in some thermokarst deposits. Numerous similar alternating sections of IC and thermokarst deposits exist along the east and west coast of the Bykovsky Peninsula. The outcrop section B–S on the northern end of the peninsula consists of 22 m of ice-rich silty IC sediments with plant remains and peat inclusions of the Zyryan and Sartan periods (Fig. 8). The cryotexture is lens-like reticulated. The IC was covered discordantly by 3 m of sandy sediments with thin organic interlayers dated as the late Sartan and representing an aquatic, probably shallow fluvial deposit.
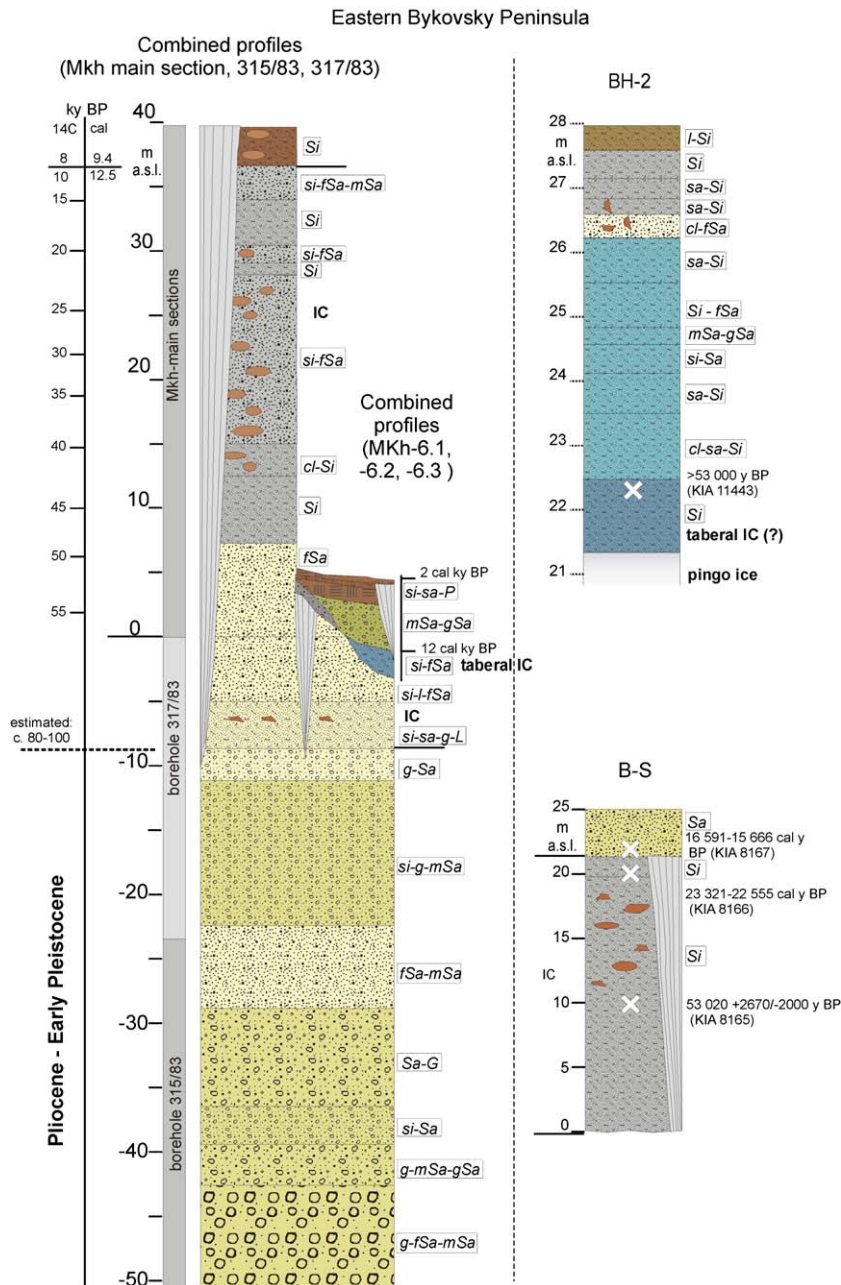
Fig. 8. Schematic sedimentological profiles for outcrops in the eastern part of the Bykovsky Peninsula: combined profile for the Mamontovy Khayata Ice Complex key site and the adjacent thermokarst depression (MKh main Ice Complex sections, MKh-6 alas sections, and boreholes 317/83 and 315/83) (Kunitsky, 1989; Schirrmeister et al., 2001); a sediment core from top of a pingo (BH-2); and a section from the northeastern shore (B–S). For profile locations see Fig. 4. The legend is shown in Fig. 6.

In the pingo-borehole BH-2 (Fig. 4), 6.5 m of sediment between 21.3 and 28 m a.s.l. were cored (Fig. 8). Directly above the ice core, 1.1 m of silty sediments occur. The sediments are probably taberal material from a former talik, and they are probably Zyryan or early Karginsky IC deposits, suggested by an infinite dating age of >53 ky BP

at 5.7 m depth. The taberal deposit has been formed below a thermokarst lake, in which silty and sandy sediments have been deposited. An interlayer of medium-grained sand with cross-beddings, plant remains, and peat inclusions indicates the influence of running water and the reworking of material. The uppermost 1.8 m are peaty,

Table 3
Remotely sensed surface structures and their indication for certain processes and periods of landscape development

Observed structures	Process indication and/or associated landscape stage
Mainly in the Khorogor Valley	
Nival cirques and cryoplanation terraces	Large perennial snowfields, névés, and extensive nivation during the Late Pleistocene
(Perennial) snow patches	Recent active nivation
Dells	Holocene sediment transport by slope wash/supra-permafrost drainage; in the upper valley they occur on slopes with thick ice-rich sediment, which probably are remains of the Late Pleistocene valley filling
Braided drainage nets	Late Holocene sediment transport by slope wash
Streams	Holocene sediment transport by fluvial activity
Oxbow lakes, inactive river channels	Late Holocene stream migration and change from fluvial to lacustrine sedimentation
Active Khorogor River delta	Late Holocene sedimentation with marine interaction
Inactive Khorogor River delta	Middle–late Holocene sedimentation; after major shift in river flow direction deactivating of the delta, changing hydrological regime
Mainly on the Bykovsky Peninsula	
Edoma uplands	Erosional remnants of the Late Pleistocene terrain surface with only minor thermokarst degradation
Thermo-erosional valleys	Holocene thermokarst and thermo-erosion above the ice wedge net
Nival niches	Late Holocene nivation at small nivation hollows in thermo-erosional valleys or thermokarst depressions with recent snow patches
Low-centre ice-wedge polygons	Middle–late Holocene refreezing of subaerial depression bottoms, formerly occupied by lakes
High-centre ice-wedge polygons	Late Holocene initial thermokarst/ thermo-erosion on slopes or on uplands
Thermokarst mounds	Late Holocene thermokarst along slopes or cliffs; presence of Late Pleistocene IC with large ice wedges
Thermo-erosional cirques and thermo-terraces	Late Holocene coastal erosion and rapid coastal retreat; presence of Late Pleistocene ice-rich IC
Large deep thermokarst lakes	Holocene thermokarst with deep subsidence
Large shallow thermokarst lakes	Holocene thermokarst without deep subsidence

Table 3 (*continued*)

Observed structures	Process indication and/or associated landscape stage
Small shallow lakes	Late Holocene meteoric or meltwater ponds; possibly initial thermokarst lakes
Thermokarst depressions	Early–middle Holocene thermokarst subsidence; sometime presence of several slope terraces indicating different stages of subsidence
Pingos	Middle–late Holocene talik refreezing; presence of Pre-Holocene coarse-grained material in the refreezing talik, climate cooling
Collapsing pingos	Late Holocene collapse of the pingo ice core, modern thermokarst
Thermokarst-lagoons	Late Holocene coastal erosion and marine inundation; Early–middle Holocene thermokarst subsidence; sea level rising
Marine lagoons and marine sandbars	Late Holocene coastal dynamics
Technogene thermokarst along vehicle tracks, roads, or constructions	Late Holocene anthropogene influence

silty–sandy sediments that were deposited under subaerial conditions.

4.2. Terrain and remote sensing analyses

4.2.1. Khorogor Valley

The catchment area of the Khorogor Valley covers approximately 365 km^2. Both the Khorogor and Khatys-Yuryakh Rivers have their sources at elevations of about 330–340 m. The Khorogor Valley can be separated into three regions (upper, central, and lower) according to surface structures and topography. The valley bottom is at 100 m a.s.l. in the upper valley, 50 m a.s.l. in the central valley, and about 5 m a.s.l. in the lower valley. The upper valley region is relatively narrow (A1–B1 in Fig. 5) and subdivided by ridges of outcropping bedrocks. The wide central to lower region is a broad valley floor with a very gentle general inclination towards the Neelov Bay in the NE, and a minor tilt towards the Khorogor River at the south-eastern valley boundary (A2–B2, A3–B3, and D–E in Fig. 5). Beside the bedrock exposures, the upper region is characterised by a steeper valley floor, moderate slopes between 2.5 and 10 degrees, cryoplanation terraces, and slope wash areas.

Table 3 gives an overview on the remotely sensed surface structures and their indication for certain

processes and periods of landscape development in the investigation area:

– The bedrock assemblage of the Khorogor Valley (alternating sandstone–silt sequences with sparse dolerite dykes) and its varying weathering resistance strongly influence the surface structures in the upper valley. The bedrock geology especially affects cryoplanation terraces, river beds, and the occurrence of a few large lakes;
– Numerous small lakes are situated in bedrock depressions at the boundary between the upper and central valleys. Step-like cryoplanation terraces with bedrock outcrops, debris fields, and patches of fine-grained sediment between them occur in higher elevations;
– Extensive slope wash areas dominate at lower slopes in the upper valley, where supra-permafrost drainage features, so-called dells, are located (Fig. 9). The generally subparallel dells occur on slopes with fine-grained ice-rich permafrost deposits, and may indicate initial thermokarst on slopes (Katasonova, 1963). Although these features can be observed with remote sensing imagery, they are hardly visible on the ground, indicating that they are not characterised by relief but by soil moisture. Almost all dells in the valley occur on slopes covered with fine-grained sediments, usually situated below 200 m a.s.l., and with slope inclinations well below 10° (Fig. 9). Similar features are sometimes described as 'rills' in western literature (e.g. Wilkinson and Bunting, 1975; Lewkowicz and Kokelj, 2002);
– The sedimentary cover over the lower and central valley bottom is usually not very thick (between 0–5 m), in contrast to sediment thickness on some slopes in the upper valley (30 m in borehole X-89). The wet tundra in the broad central valley is dominated by a large dell system with partially braided surface runoff. Thermokarst mounds occur especially along river-banks, roads, or on slopes of side valleys. The
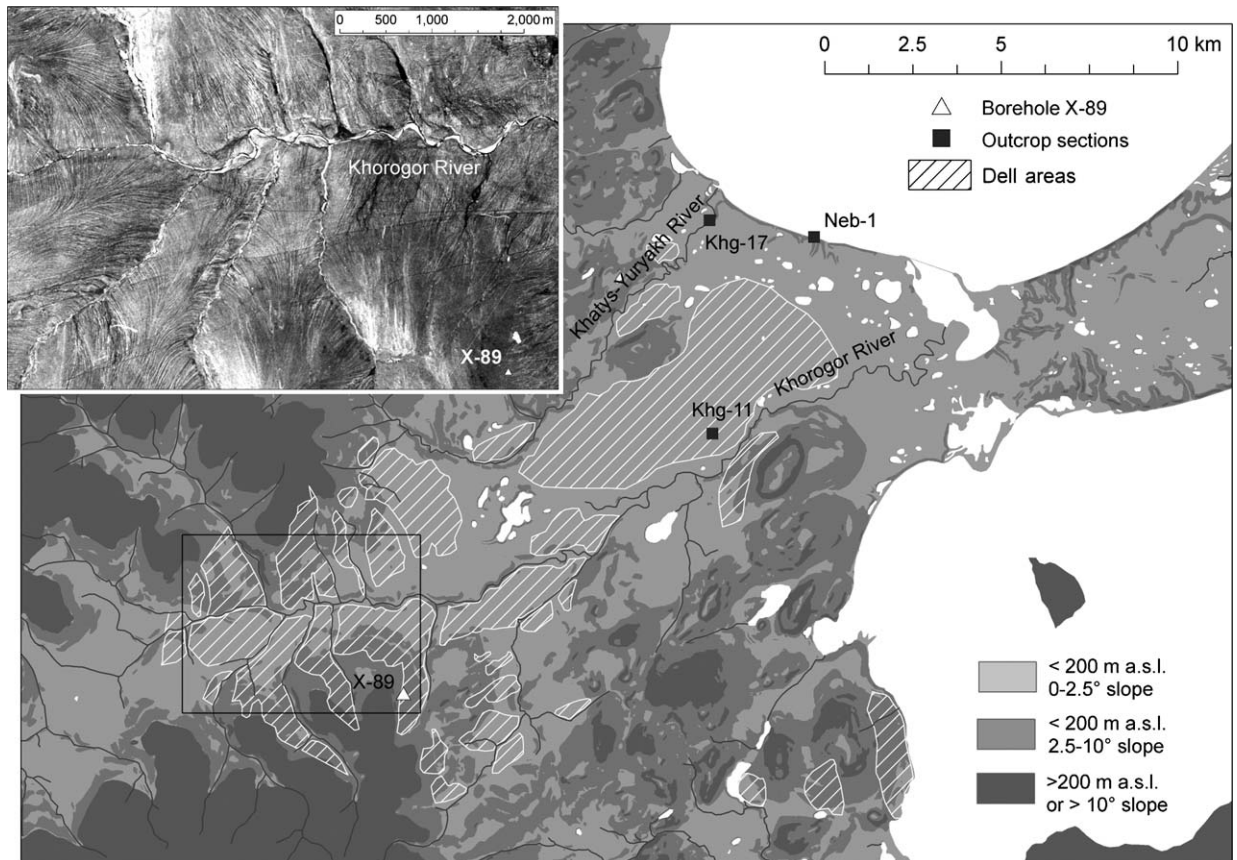

Fig. 9. Slope map of the Khorogor Valley. The majority of dells are situated in regions below 200 m a.s.l. and less than 2.5° in slope. Almost no dells occur at slopes steeper than 10°. The black box indicates the location of the Corona image subset in the upper left. Like in this image, subparallel dells are widely distributed at the slopes in the upper and central valley regions. They indicate supra-permafrost drainage in a direction of the slope towards small valleys or brooks, and the presence of fine-grained and probably ice-rich sedimentary deposits (e.g. 12 m at borehole X-89).
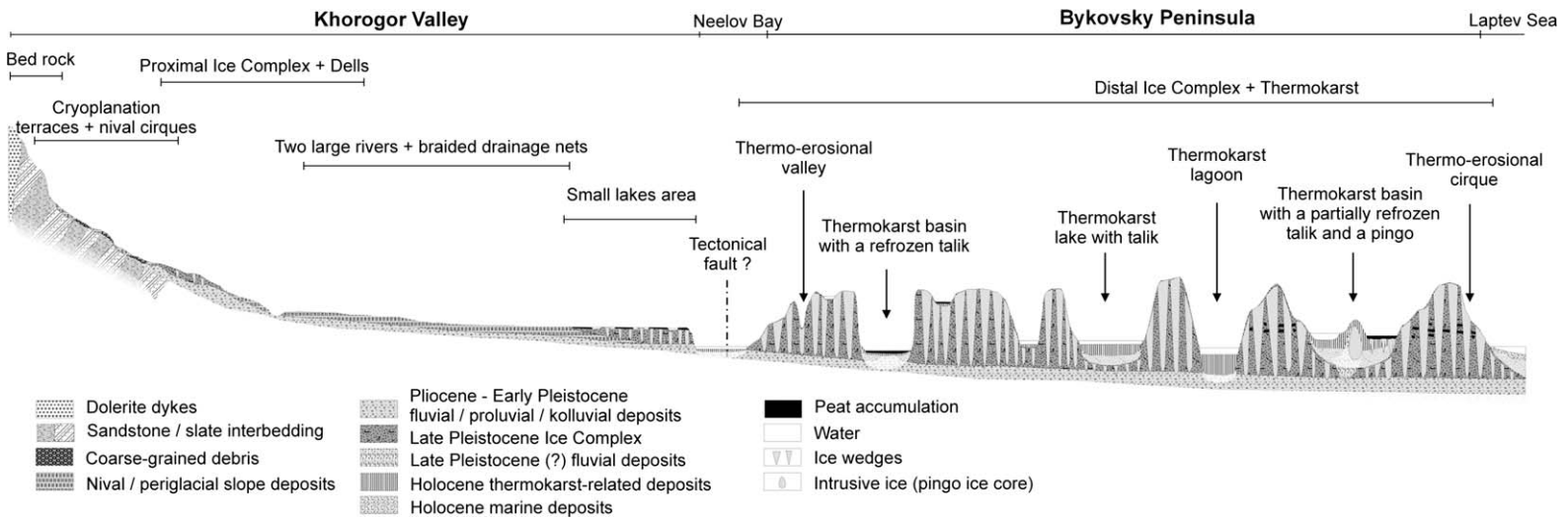
Fig. 10. Schematic cross-section of the investigation area (Schema not drawn to scale).

mounds indicate the former presence of ice-wedge polygons and thus a thicker cover of ice-rich sediment at these locations. These deposits are considered as IC-like formations. Most locations, especially in the central and lower valleys, are covered with a late Holocene to subrecent peat horizon (Fig. 6);

– A large area in the lower valley, containing assemblages of small lakes, has an extremely low inclination (lowest part of cross-section D–E in Fig. 5).

The derived information were generalized and compiled in a schematic cross-section covering the Khorogor Valley and the Bykovsky Peninsula (Fig. 10).

4.2.2. Bykovsky Peninsula

The topography of the Bykovsky Peninsula is heavily dissected (Fig. 10). The maximum elevation of the Yedoma uplands on the Bykovsky Peninsula is about 43 m a.s.l. The Yedoma in the northern and the south-eastern region have lower elevations of about 25 m due to strong erosion at these narrow parts of the peninsula (G1–G2 in Fig. 5). Generally, there are no major differences in the maximum elevation of the original Yedoma heights between the western and eastern regions of the peninsula (F1–F2 in Fig. 5).

About 46% of the peninsula consists of deep thermokarst depressions (Grosse et al., 2005). Agglomerated depressions form four major W–E oriented basins and subdivide the peninsula into Yedoma uplands. The thermokarst depressions mostly have steep slopes and very low mean elevations of 1–8 m a.s.l. The coastal areas are strongly dissected by thermo-erosional valleys (G1–G2 in Fig. 5).

The dominant structures, related processes, and their indications for different landscape development stages are summarised in Table 3.

The Bykovsky Peninsula consists of landscape elements representing at least eight major stages:

– The oldest observable surface features are the Yedoma uplands. They consist of the syngenetically frozen IC deposits, indicating continuous permafrost aggradation during this *stage 1*.
– The next *stage 2* is characterised by permafrost degradation in the form of thermokarst depressions dissecting the Yedoma. The development of an extensive network of thermo-erosional valleys started with the thermokarst subsidence.
– Presently, thermokarst lakes in the depressions are apparently smaller than the depressions (Grosse et al., 2005). Thus, *stage 3* with maximum lake extent and subsequent *stage 4* with massive lake drainage can be

inferred. Stage 4 is marked by the formation of wide terraces in the depressions and peat bogs.

– The following *stage 5* is characterised by permafrost aggradation again, expressed by pingo growth above refreezing lake taliks and the growth of ice wedge polygonal networks in drained thermokarst depressions.
– In *stage 6*, thermokarst depressions are truncated by coastal erosion. This formation of thermokarst lagoons by marine ingression indicates enhanced coastal dynamics resulting from the global marine transgression. Thermo-erosional cirques along some Yedoma coastal cliffs also belong to this stage.
– Two final *stages 7/8* of local importance can be inferred from the isthmus where the peninsula is connected to the mainland. Here the Khorogor River first formed a delta in the Safroneeva lagoon south of the small isthmus (Fig. 3). A shift in the river course to the north deactivated this delta by cutting water and sediment supply. A second and still active delta formed afterwards in the Stepanenko thermokarst lagoon north of the isthmus.

5. Phases of landscape evolution and their implications

Like in most geological–geomorphological investigations, field data is heterogeneously distributed in our investigation area. Our interpretation of the stratigraphy, and thus reasoning for the landscape genesis scheme, was built on the presently available amount of sedimentological, cryological, palaeontological, geochronological, and geomorphological data. Of course, the presented data of this study has an interpretative character, and limitations in the study resulting from the heterogeneous data distribution are debatable. Nevertheless, we are confident that this rather complex approach based on the best available data resources and previous scientific results successfully describes the major geological and geomorphological evolution of this region during the Late Quaternary.

5.1. Pliocene to Early Pleistocene

According to Imaev et al. (2000), the Kharaulakh Ridge experienced a major linear uplift during the late Oligocene to the Early Pleistocene. As a result, the landscape was dominated by strong fluvial activity during a period interpreted as Pliocene to the Early Pleistocene by Kunitsky (1989) and Grigoriev (1993) (Fig. 11). The rivers transported large amounts of medium to coarse sands and rounded gravels over wide distances from the Kharaulakh Ridge in the west to the
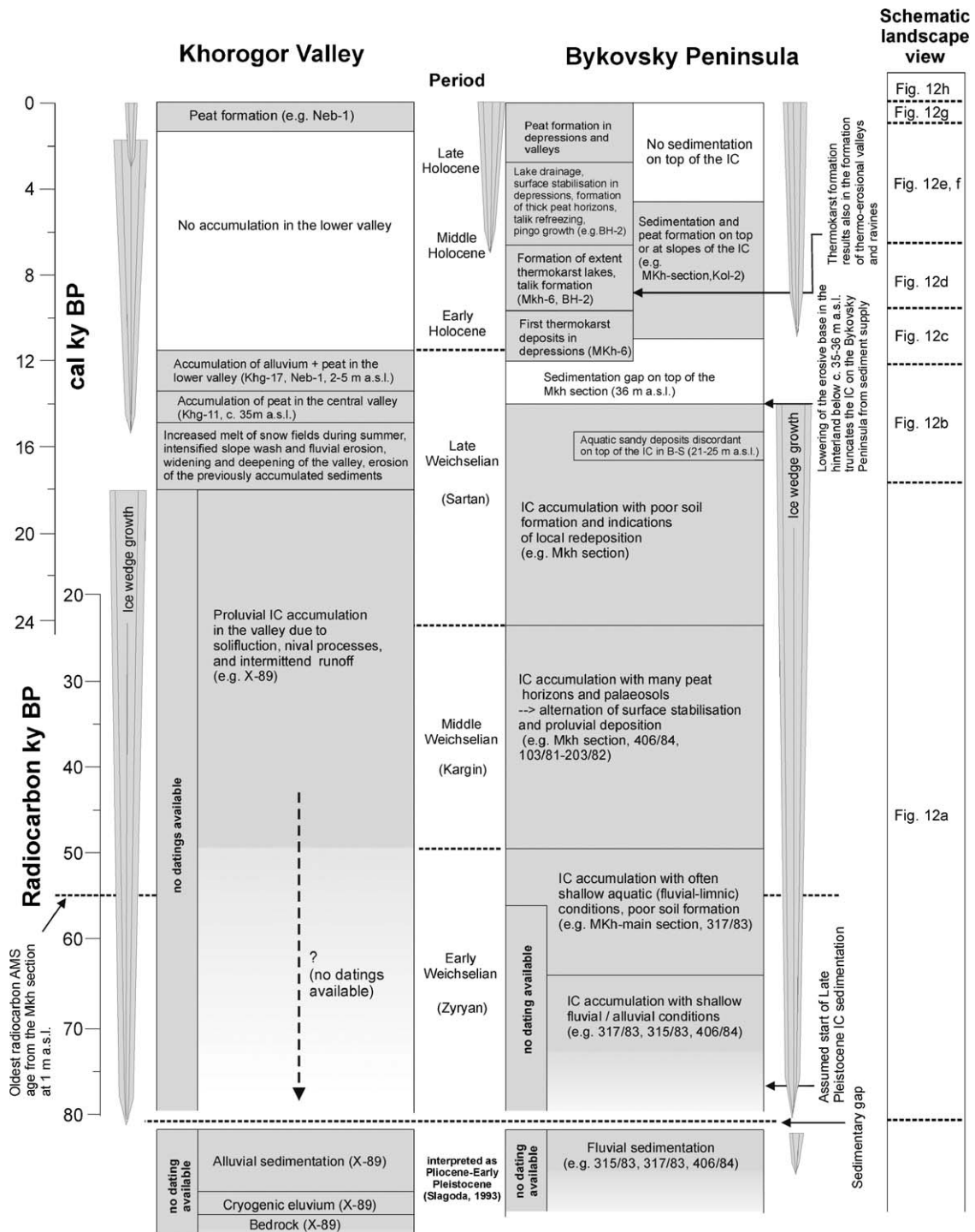
Fig. 11. Schema of periglacial facies development in the studied landscape complex.

mountain foreland in the east. These deposits were evident in 21 boreholes on the western and eastern Bykovsky Peninsula (e.g. 406/84 in Fig. 7; 317/83 in Fig. 8), but also several km offshore the Bykovsky Peninsula (e.g. 315/83 in Fig. 8) and Muostakh Island. Fluvial deposits below the Bykovsky Peninsula were detected from 9 m to >51 m b.s.l. Plant remains, such as grass roots and shrub twigs frozen in the sediments,

prove that the region had a vegetation cover during this period. The sporadic occurrence of coal detritus indicates the change of the sediment origin, and thus varying river source areas. Coal-bearing deposits for instance occur in the Tertiary Sogo Graben several km south of the Bykovsky Peninsula (Fig. 1). After this
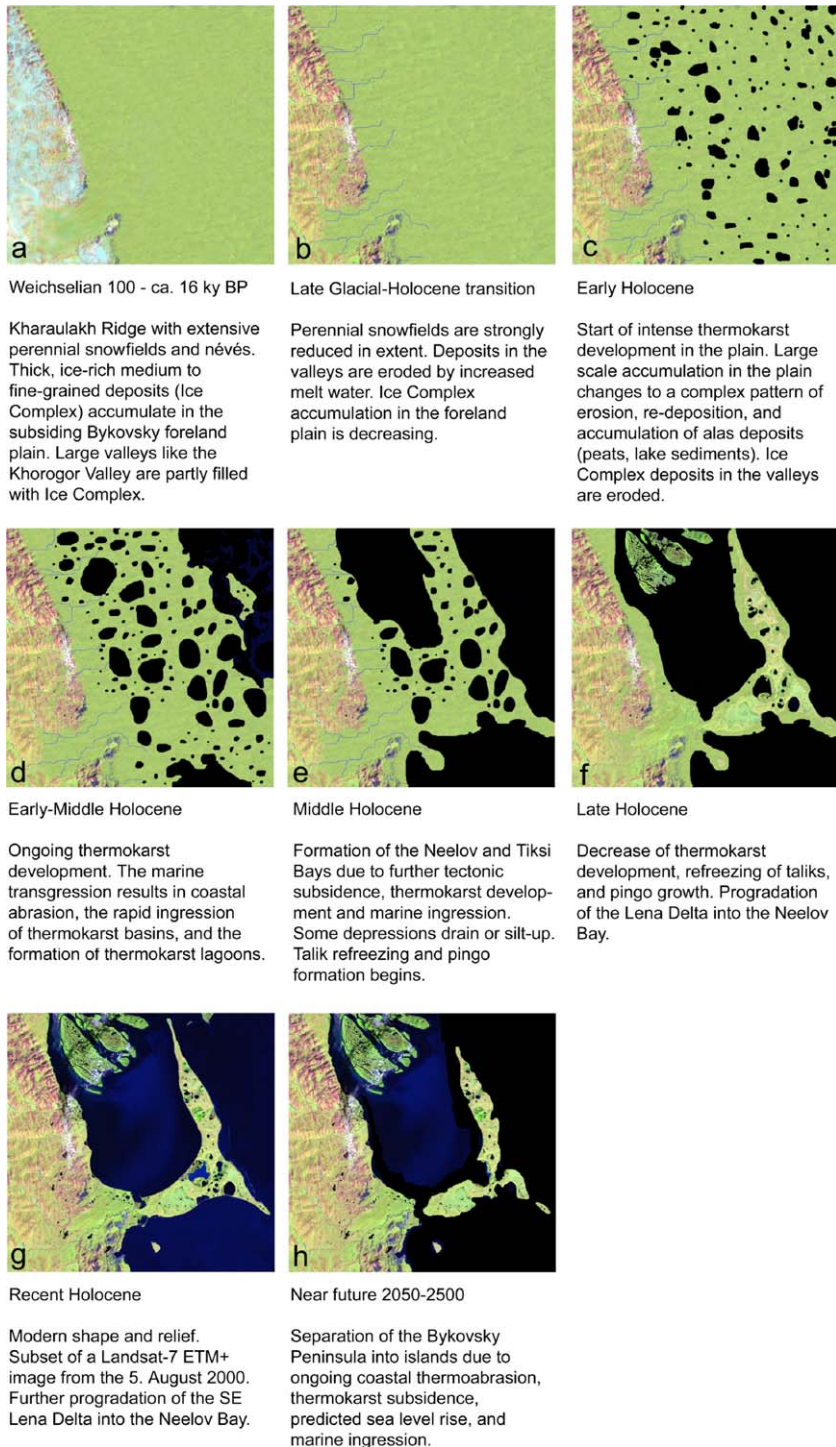

a
Weichselian 100 - ca. 16 ky BP

Kharaulakh Ridge with extensive perennial snowfields and névés. Thick, ice-rich medium to fine-grained deposits (Ice Complex) accumulate in the subsiding Bykovsky foreland plain. Large valleys like the Khorogor Valley are partly filled with Ice Complex.

b
Late Glacial-Holocene transition

Perennial snowfields are strongly reduced in extent. Deposits in the valleys are eroded by increased melt water. Ice Complex accumulation in the foreland plain is decreasing.

c
Early Holocene

Start of intense thermokarst development in the plain. Large scale accumulation in the plain changes to a complex pattern of erosion, re-deposition, and accumulation of alas deposits (peats, lake sediments). Ice Complex deposits in the valleys are eroded.

d
Early-Middle Holocene

Ongoing thermokarst development. The marine transgression results in coastal abrasion, the rapid ingression of thermokarst basins, and the formation of thermokarst lagoons.

e
Middle Holocene

Formation of the Neelov and Tiksi Bays due to further tectonic subsidence, thermokarst development and marine ingression. Some depressions drain or silt-up. Talik refreezing and pingo formation begins.

f
Late Holocene

Decrease of thermokarst development, refreezing of taliks, and pingo growth. Progradation of the Lena Delta into the Neelov Bay.

g
Recent Holocene

Modern shape and relief. Subset of a Landsat-7 ETM+ image from the 5. August 2000. Further progradation of the SE Lena Delta into the Neelov Bay.

h
Near future 2050-2500

Separation of the Bykovsky Peninsula into islands due to ongoing coastal thermoabrasion, thermokarst subsidence, predicted sea level rise, and marine ingression.

Fig. 12. Schematic view of major phases of Late Quaternary landscape evolution southeast of the Lena Delta, based on a Landsat-7 ETM + image and its manipulation.

fluvial phase a large sedimentary gap exists until the beginning of the Late Pleistocene in the whole region.

5.2. Late Pleistocene (Weichselian)

During the entire Weichselian (Zyryan, Karginsky, and Sartan), a wide accumulation plain developed in front of the Kharaulakh Ridge (Figs. 11 and 12a), probably enhanced by tectonic subsidence in the foreland. A major factor for the beginning of IC accumulation during the Weichselian was probably the growth of a large Early Weichselian ice sheet over Northern Europe and Western Siberia (Svendsen et al., 2004). The ice sheet blocked the transport of moisture from the Atlantic to north-eastern Siberia and resulted in an increased aridity in these regions, which is documented in a variety of environmental proxies for the Bykovsky Peninsula, e.g. pollen (Andreev et al., 2002), plant macro remains (Kienast et al., 2005), or insect remains (Sher et al., 2005). Low precipitation rates prevented ice sheet growth in the Laptev Sea region, thus the surrounding low mountain ranges were not covered by a large ice sheet during that time (Hubberten et al., 2004). Nevertheless, extensive perennial snowfields and névés existed in these mountains (Galabala, 1997). As a result, the supply of water was probably much smaller during most times of the year except during the snowmelt, leading to intermittent and strongly seasonal sediment deposition. The high continentality with severe winters resulted in intensive nival weathering and erosion connected to the formation of cryoplanation terraces and nival cirques in the Kharaulakh Ridge. Large perennial snowfields accumulated in these structures, and nival weathering products were deposited with the snow. Aeolian deposition also occurred on these snowfields, as it was widespread on the Eurasian continent during the Late Pleistocene (e.g. Rutter et al., 2003). Nevertheless, there are no pure Late Weichselian aeolian deposits in the region, which can be inferred from the generally polymodal grain size distribution curves of the IC (Siegert et al., 2002). The quite warm summers (Kienast et al., 2005) resulted in intense snowmelt, strongly increased slopewash and solifluction downslope of the snowfields. The nival and aeolian sediments from snowfields were redeposited then in the lower valley and subsequently transported to the accumulation plain. Slopewash and solifluction was enhanced by a permafrost table close to the terrain surface that prevented the deep drainage of meltwater and resulted in suprapermafrost and above-surface drainage, and the increase of solifluction rates. Solifluction on permafrost grounds, so-called gelifluction, already begins at slope angles as low as 1–3° and is strongly dependent on the water content in the active layer (French, 1996). Many studies from periglacial regions have shown that snowmelt has a larger impact on slope and surface erosion than summer precipitation (e.g. Lewkowicz, 1981; Stromquist, 1985). Additionally, during the Weichselian the vegetation cover was probably much more fragmentary in the higher, colder and more wind-exposed zones of the Kharaulakh Ridge, making the surface sediments more prone to erosion. The surface wash in the Kharaulakh Ridge resulted in erosion and transport of fine-grained nival and aeolian sediments from snowfields and slopes towards the valleys. Similar processes, but in a smaller scale, were observed in the vicinity of present-day snowfields in the Kharaulakh Ridge and other mountain ranges in the Laptev Sea region (Kunitsky, 1989; Kunitsky et al., 2002; Schirrmeister et al., 2003). The dells are such drainage features on periglacial slopes with sedimentary cover and poor drainage conditions (Fig. 9). Although the dells themselves are of Holocene age, they indicate the presence of relatively thick ice-rich sediments in the upper valley. We assume that comparable features developed in a much larger scale in the Late Pleistocene valleys of the Kharaulakh Ridge. The highly seasonal runoff since the Zyryan Glacial was not capable of eroding and transporting all the periglacial weathering products and aeolian sediments from the mountains to the foreland plain, thus the valleys became slowly filled with sediments. We suggest that the sediments occurring in core X-89 are erosive remnants of a Weichselian sedimentary filling in the Khorogor Valley, at least several metres thick (Fig. 6). The geocryological facies were very similar to that on the foreland plain, although these proximal deposits have generally coarser grain sizes. The ground ice content is very high and comparable to that of the Bykovsky Peninsula IC. Ice wedges are also present in these deposits. Beyond their indication for cold-climatic conditions they also suggest a hydrology and geomorphology favourable for ice wedge growth in the upper valley. Large syngenetic ice wedges preferably grow in areas with low or no slope inclination. Even small slope inclinations lead to solifluction in fine-grained permafrost sediments (French, 1996), which prevents the growth of large ice wedges. This suggests smoother relief conditions than present in the upper valley during that period, resulting from the massive sedimentary filling of the valley. Thus, we propose that IC-like sediments were also accumulated in the Khorogor Valley during the Weichselian. The general pattern of sedimentation was relatively stable during the whole Weichselian.

5.2.1. Early Weichselian Glacial (Zyryan)

The accumulation of the Zyryan IC started at about 80 ky BP (Fig. 11) (estimated by Meyer et al., 2002a), and resulted in 12–17 m thick ice-rich sediments. The fluvial energy was apparently much lower than that during the Early Pleistocene, as this first stage of IC sedimentation was dominated by episodically shallow fluvial or alluvial floodplain-like facies with silty to fine-grained sandy deposits with graded bedding (406/84 in Fig. 7; MKh main section of 317/83 in Fig. 8). The interpretation of floodplain sedimentation is supported by lithological analyses indicating only weak soil formation in contrast to the upper part of the section (Slagoda, 1993, 2004). The Zyryanian deposits occurred in numerous boreholes and outcrop sections on the Bykovsky Peninsula. Their elevation at Mamontovy Khayata is between 9 m b.s.l. and 8 m a.s.l. Large syngenetic ice wedges grew in these deposits and formed polygonal ground. Stable isotopes in these ice wedges indicate severe winter temperatures (Meyer et al., 2002a).

We propose that the Kharaulakh Ridge and the Khorogor Valley are main sedimentary sources for the Bykovsky Peninsula IC. A high content of redeposited pre-Quaternary Pinaceae pollen especially in the Zyryan and Sartan IC sequence (Andreev et al., 2002) indicates the origin of the sediments in the nearby mountains of the Kharaulakh Ridge, where such pre-Quaternary deposits with Pinaceae pollen occur (Grinenko et al., 1998). Analyses of heavy minerals and rock fragments show the mineralogical similarity of Kharaulakh bedrocks with various Late Pleistocene sediments in the Khorogor Valley and the Bykovsky Peninsula IC deposits (Siegert et al., 2002) and recent sediments in the Khorogor Valley. Similar results were obtained from investigations of mountain ranges and foreland IC in the Chekanovsky Ridge southeast of the Lena Delta (Schwamborn et al., 2002; Schirrmeister et al., 2003) and from Bol'shoy Lyakhovsky Island (Kunitsky et al., 2002), suggesting a strong genetic relationship between the mountain ranges and the foreland IC.

5.2.2. Middle Weichselian Interstadial (Karginsky)

The IC accumulation in the foreland plain reached a certain elevation level (9–22 m a.s.l. at Mamontovy Khayata) and thus the inclination and relief energy of the accumulation plain became too low for middle- to coarse-grained fluvial sedimentation. The sedimentation changed to more proluvial, periodic deposition (Fig. 11). A strong climatic seasonality persisted, thus the highly seasonal runoff continued and mainly silty to fine-grained sandy sediments were deposited in the accumulation plain. Approximately 12–15 m of sediment were accumulated at the Mamontovy Khayata section during the Karginsky or 50–28 ky BP (Fig. 8). The environmental conditions were rather variable and the drainage of the tundra plain became poorer (Schirrmeister et al., 2002a). Well-developed palaeocryosol formation and intensive peat growth during the Karginsky are evident in almost all analysed profiles. The general geocryological conditions did not change, and syngenetic ice wedges continued to grow (Meyer et al., 2002a).

5.2.3. Late Weichselian Glacial (Sartan)

The IC of the Sartan was characterised by continuous proluvial sedimentation and local redeposition of fine-grained material in the poorly drained polygonal tundra plain in the Bykovsky Peninsula area (Fig. 11). The climatic conditions were generally more arid than now (e.g. Hubberten et al., 2004) and dominated by strong seasonal temperature differences (Schirrmeister et al., 2002a). This resulted in a decrease of soil formation (Schirrmeister et al., 2002a) and the continuous growth of syngenetic ice wedges (Meyer et al., 2002a). With the accumulation of 13–15 m Sartanian IC deposits, the highest IC elevation was reached in the region of the Mamontovy Khayata site. A modelled virtual accumulation plain plotted through the highest Yedoma elevations (40–43 m a.s.l.) reveals a small inclination of this plain. As the proposed main sediment source was the Kharaulakh Ridge, we assume that the Khorogor Valley was filled completely with IC-like deposits to at least similar elevations during the Sartan. Even the higher parts of the valley were partially filled with ice-rich deposits at least several metres thick, as is documented by the 15 m thick IC-like sediments in core X-89 at 160 m a.s.l. (Fig. 6), which were correlated with the Sartan (Slagoda, 1993). In the central and lower valleys only IC-like deposits of the Bølling/Allerød were found above weathered bedrock or cryogenic eluvium between 36 m a.s.l. (Khg-11) and 2.5 m a.s.l. (Neb-1). This means that large parts of the original IC filling within the Khorogor Valley were removed before the Bølling/Allerød. The continuous IC accumulation on the Bykovsky Peninsula ended between 12.5–13 cal ky BP (Fig. 13), which coincides approximately with the end of the Bølling/Allerød climatic period.

5.2.4. Late Glacial–Holocene transition

Major landscape changes occurred during the late Sartan and early Holocene, probably triggered by the beginning of climate amelioration. An important factor was probably the increase of solar insolation on the northern hemisphere and an insolation maximum around 10–12 ka BP due to the orbital parameters
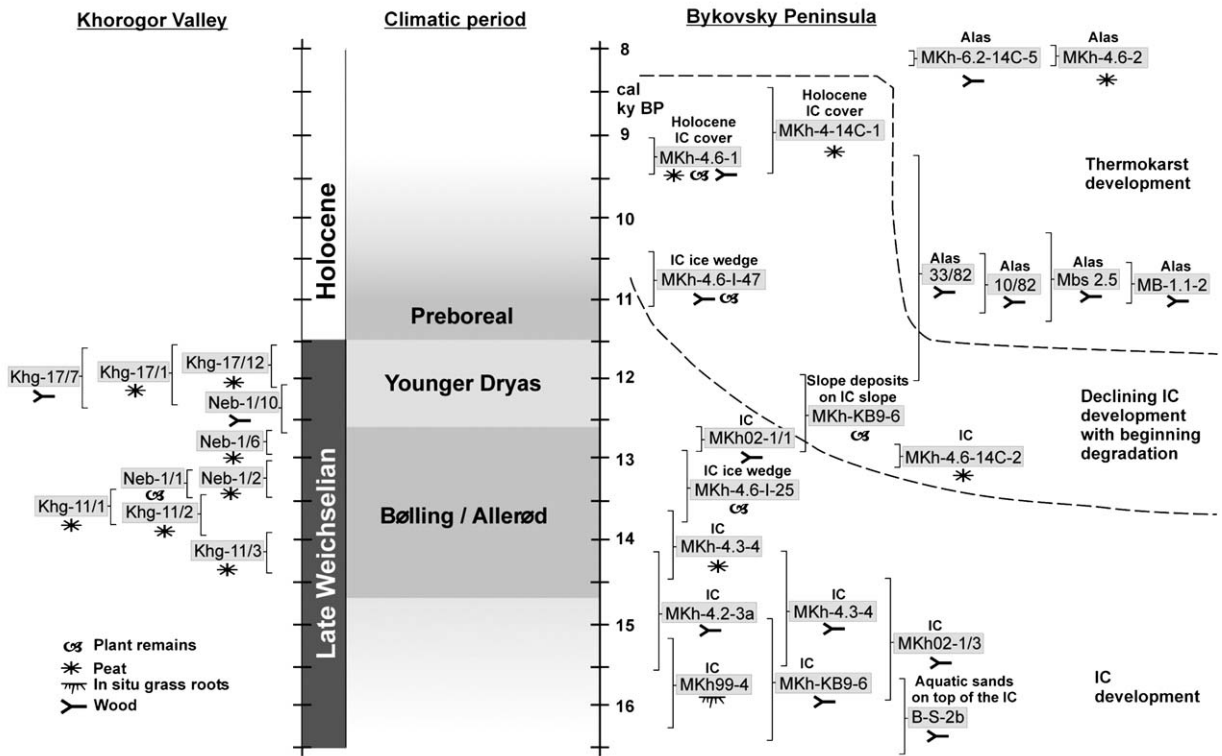
Fig. 13. Calibrated radiocarbon dates covering the transition period between the Late Pleistocene and the early Holocene in the investigation area. The vertical bar for each dating indicates the 2-σ error range. The datings are from Table 1, Schirrmeister et al. (2002b), and Meyer et al. (2002a). The boundaries of the climatic periods are based on Greenland ice core data after Dansgaard et al. (1993).

(Berger and Loutre, 1991). This resulted in an about 10% higher mid-month June insolation at 70° N than in the preceding Middle and Late Weichselian. Climatic changes in the region are associated with a shift of the major winter precipitation source, as recorded in stable isotope compositions of late Sartan ice wedges (Meyer et al., 2002a). Other indicators are the increase of herbs and a generally denser vegetation between ca. 18 and 14 cal ky BP, as inferred from pollen spectra (Andreev et al., 2002). For the Allerød, Velichko et al. (2002) derived a +2 °C higher July temperature compared to the present one in this region from spatial climatic reconstructions based on North Eurasian pollen analyses. Insect assemblages of the late Sartan IC at Mamontovy Khayata indicate a sharp rise in summer temperatures and high aridity for the same period (Sher et al., 2005). Additionally, the number of dated mammoth remains from the Laptev Sea region has a distinct rise in this period after a steady decrease over the preceding 10 ky (Sher et al., 2005).

The climate amelioration led to a more extensive melting of snowfields in the Kharaulakh Ridge and resulted in increased discharge rates of melt water

(Figs. 11 and 12b). The Khorogor Valley has the largest catchment area in the region, thus the discharge of meltwater from snowfields and névés through the valley must have been quite high. That not only caused intensified slopewash but also fluvial erosion of the IC-like deposits that were previously (earlier than Bølling/Allerød, which is ca. 12.6–14.6 cal ky BP) accumulated in the valleys. Evidence for increased discharge rates during this period are shallow fluvial sands found in a section of the northern Bykovsky Peninsula (profile B–S in Fig. 8). They discordantly overlay the IC, and their base was radiocarbon-dated to 16.6–15.7 cal ky BP (Table 1).

The idea on the filling and subsequent erosion in the Khorogor Valley is supported by Gravis (1969a,b), who intensively investigated periglacial slope processes in the NE Siberian Kular Range southeast of our investigation area. He assumes that the intensity of periglacial slope processes such as slope wash and solifluction depends on climatic conditions. Gravis (1969a,b) established a rhythmic sequence for the investigated Late Pleistocene deposits, whereas each glacial and interglacial period was divided into two phases of slope processes. During the first phase, valleys

were mostly filled with sedimentary material, while during the second phase, the valley infill was mostly eroded, and valleys deepened. Generally, the deepening and erosion was stronger during the interglacials.

The erosion in the central Khorogor Valley stopped around ca. 14.4 cal ky BP, when thin alluvial sediments above weathered bedrock were covered with a 1 m thick peat horizon. Synchronously, alluvial sands with peat inclusions were accumulated in the lower valley and polygonal ice wedge systems formed on the valley floor (sections Khg-11, Khg-17, and Neb-1 in Fig. 6). Pollen records from these sediments (Fig. 14) suggest dense
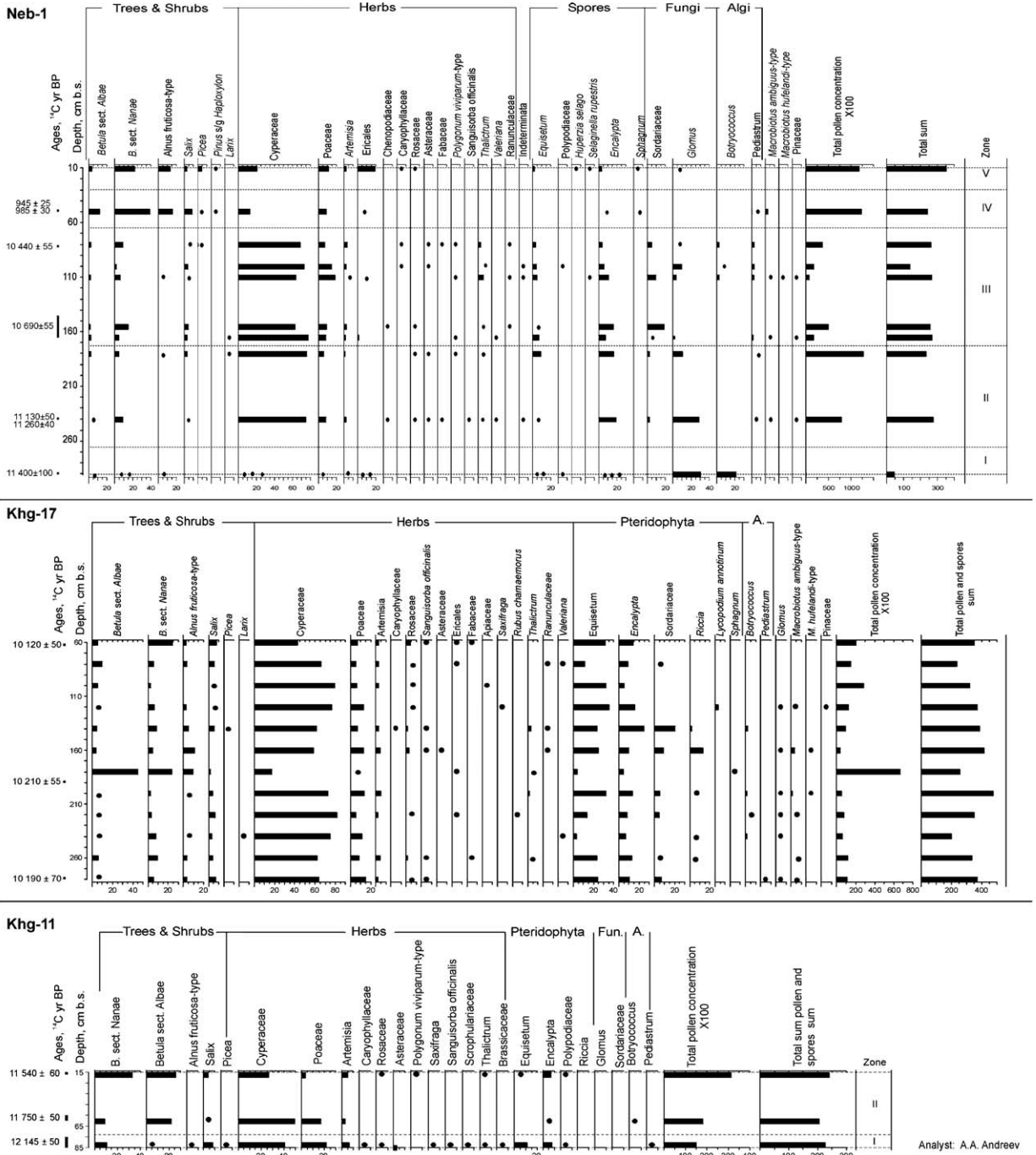
Fig. 14. Pollen diagrams from the Khorogor Valley sections Neb-1, Khg-17 and Khg-11.

grass and shrub vegetation (*Cyperaceae, Poaceae, Betula nana* and *Salix*) in the valley, and thus an ameliorated climate correlated to the Bølling/Allerød.

Palynological data from the Neb-1 site reflect the presence of disturbed soils, probably due to a more exposed position of the site at the valley mouth. The presence of large epigenetic ice wedges indicates relative stable surface conditions probably during the following Younger Dryas cold period. Pollen zone III of Neb-1 and the lower sediments of Khg-17 (Fig. 14) have lower pollen concentrations. They are characterised by *Equisetum*, which is an indicator of disturbed soils, and contain high amounts of dung-inhabiting Sordariaceae spores, which probably may indicate the presence of grazing herds in the region during the Younger Dryas. Pollen spectra from the middle part of Khg-17 are noticeable for dramatic increase in *Betula nanae*, *B. albae* and *Alnus fruticosa* pollen amounts. Such increase documents an abrupt climate amelioration at the Late Glacial/Holocene transition. The upper two spectra from the Neb-1 section reflect the late Holocene palaeo-environment close to the modern one.

The landscape development in the Khorogor Valley and the Bykovsky accumulation plain appears clearly disconnected already before the Bølling/Allerød. Contemporary deposits are located 20–35 m higher on the Bykovsky Peninsula than in the lower Khorogor Valley within a short distance of only 10–20 km. The supposed erosion in the Khorogor Valley resulted in a lowering of the valley bottom and therefore a weaker sediment supply on the accumulation plain in about 35–40 m a.s.l. The local hydrological regime of the Bykovsky accumulation plain became slowly disconnected from the Kharaulakh Ridge. Locally, the IC accumulation continued during this time, such as at the Mamontovy Khayata site. Between ca. 12.5 and 9.4 cal ky BP a sedimentation gap occurs near the top of the Mamontovy Khayata permafrost sequence at 36.5 m a.s.l., as is evident from radiocarbon dates (Table 1 and Schirrmeister et al., 2002b; see also Figs. 8 and 13). This gap coincides with the beginning of local thermokarst processes that totally reorganized the hydrological regime. The thermokarst development finally had disconnected the Bykovsky accumulation plain from the main sediment supply in the Kharaulakh Ridge, and resulted in the termination of major sedimentation on the top of the Bykovsky Peninsula IC at the end of Bølling/Allerød. The massive landscape dynamics in the investigation area during the Late Glacial–Holocene transition appear synchronous with a peak of freshwater input from an unidentified source to the Laptev Sea detected in a marine sediment core from the Laptev shelf (Spielhagen et al., 2005).

5.3. Early Holocene

The strong climatic warming and increase of precipitation in the region during the early Holocene is well-documented in a wide range of palaeo-environmental proxies in the Mamontovy Khayata sequence and adjacent thermokarst deposits (Andreev et al., 2002; Schirrmeister et al., 2002a; Bobrov et al., 2004; Sher et al., 2005). Ice wedge growth was limited in this period (Meyer et al., 2002a). In an initial stage, probably at around 12 cal ky BP, the higher humidity and the poor drainage conditions resulted in the formation of water bodies in shallow relief depressions in the flat accumulation plain (Fig. 12c). These ponds rapidly increased in size, resulting in self-enforcing thermokarst subsidence due to the redirection of runoff towards the deepening depressions. This initial phase of thermokarst subsidence and lake growth must have happened very rapidly, as well-developed thermokarst deposits appear already at ca. 11.5 cal ky BP on the Bykovsky Peninsula (Fig. 13; Schirrmeister et al., 2002b). Assuming a total thermokarst subsidence of 35–45 m within 500 years (e.g. MKh-6 in Fig. 8), a subsidence rate of about 7–9 cm year^{-1} can be calculated for this period. Modern thermokarst subsidence rates for disturbed sites in Central Yakutia are 17–24 cm year^{-1} (Fedorov and Konstantinov, 2003). The landscape became strongly dissected during the early Holocene and local sedimentary processes around the thermokarst depressions dominated. Unquestionably, this climatic and geomorphic change had a strong influence on local ecology, e.g. by generating wind-protected habitats in depressions and valleys with shrub and tree tundra vegetation, or by favouring wetness-adapted plants.

The rapid subsidence of thermokarst depressions and the formation of steep slopes resulted in the massive reworking of IC material by solifluction and slope wash, and the deposition of fine- to coarse-grained subaerial deposits (combined profile MKh-6 in Fig. 8). Lacustrine silty–sandy deposits were accumulated in thermokarst lakes. They are located directly above the IC deposits, which have been turned into typical taberal sediments due to talik formation below the lake (pingo sediment core BH-2 in Fig. 8). The thermokarst development climaxed in the Early Holocene Optimum, when thermokarst lakes reached their maximum extent in the region around ca. 7–5 cal ky BP (Figs. 11 and 12d). Some depressions coalesced by lateral extension and formed large basins crossing the entire peninsula from west to east. We suggest that these basins formed at locations where the thermal, hydrological, and sedimentological properties were especially favourable for massive thermokarst, e.g. due to the former presence of

shallow stream valleys that possibly drained the accumulation plain from west to east during the Weichselian. An indicator for this hypothesis is the presence of coarse-grained sands with graded bedding in the sediment sequences of some thermokarst depressions (e.g. MKh-6 and BH-2 in Fig. 8).

The subsidence of large depressions was accompanied by the formation of thermo-erosional valleys, which mostly developed above the Late Pleistocene ice-wedge network. These extensive valley networks often radially drained the remaining IC uplands (Yedoma) towards existing depressions. Yedoma with negligible or poor drainage conditions were disturbed locally by small-scale thermokarst features, which deposited peat-rich sediments on top of the IC since ca. 9.4 cal ky BP.

5.4. Middle–late Holocene

After the Early Holocene Optimum, a climate deterioration is indicated by the declining thermokarst development, the drainage or silting-up of thermokarst lakes, and the refreezing of lake taliks (Fig. 11). Other proxies that suggest climate deterioration are the decreasing content of tree pollen (Andreev et al., 2002) and the restart of ice wedge growth in subaerial thermokarst depressions and thermo-erosional valleys (Meyer et al., 2002a). Two phases of surface stabilisation are connected with peat formation in depressions and valleys at ca. 6–3 cal ky BP and ca. 1.5–0.9 cal ky BP (Table 1; Schirrmeister et al., 2002b). In the Khorogor Valley the youngest peat (ca. 0.8 cal ky BP) was identified at the valley mouth (Neb-1 in Fig. 6). Initial thermokarst formed several shallow small lakes in the lower Khorogor Valley during the latest Holocene.

The presence of several pingos on the Bykovsky Peninsula proves the refreezing of lake taliks due to lake drainage. Approximately around 5 cal ky BP the Laptev Sea transgression reached its Holocene high-stand (Bauch et al., 2001). The presently observed thermo-erosional cirques along the shore are significantly younger. According to Rachold et al. (2003), the average coastal retreat at the ice-rich coasts of the Laptev and East Siberian Seas is about 2.5–3 m year^{-1}. Assuming a relatively stable rate, the coastal retreat by thermo-abrasion during the last 5 ky amounts 12.5 to 15 km. Thermokarst lagoons were formed due to coastal erosion and marine inundation of thermokarst depressions during the late Holocene (Fig. 12e). This development is exemplary for large parts of the Laptev Sea shelf (Romanovskii et al., 2004).

The modern shape of the Neelov Bay and the Tiksi Bay has formed during the middle–late Holocene by IC erosion and inundation of thermokarst depressions (Fig. 12e–g). The Bykovskaya Channel, a major outlet from the Lena Delta, is directed towards the Neelov Bay and probably played an important role for IC erosion and inundation in this region.

The Khorogor River accumulated a delta in the Safroneeva Lagoon south of the isthmus during the late Holocene. The deactivation of this delta due to riverbed shifting occurred probably in subrecent times. Since then the still active delta is prograding in the Stepanenko Lagoon north of the isthmus. Possible causes in this low relief area could be neotectonics in the region of the isthmus, or the blocking and redirecting of the river by ice and sediment jams during a major spring melt flood. This demonstrates that even small geomorphic changes caused by thermokarst subsidence, neotectonics, or river ice-jams can have a large effect on the depositional pattern in such flat tundra landscapes. The landscape development of the region in the near future will be dominated by the separation of the peninsula into several islands by global sea level rise, active coastal erosion, ongoing thermokarst, and marine ingression of thermokarst depressions (Fig. 12h), a process that led already to the formation of Muostakh Island in the SE (Fig. 1).

6. Conclusions

The development of the accumulation plain in the foreland of the Kharaulakh Ridge was closely connected to climatically controlled periglacial sedimentary processes and tectonic activity in the mountains. During a period of tectonic uplift in the Pliocene and Early Pleistocene the landscape was dominated by strong fluvial activity. Between the Early Pleistocene and the Weichselian a sedimentary gap developed in the region.

The IC sedimentation during the Weichselian was closely connected to periglacial processes in the nearby Kharaulakh Ridge. The highly continental climate during this period, characterised by a strong seasonality of air temperatures and hydrology, appears to be a precondition for the accumulation of fine-grained, ice-rich IC deposits in the mountain valleys and the foreland. Extensive perennial snowfields or névés in the mountains resulted in nival processes, seasonal slopewash and solifluction, and seasonal active melt water brooks, providing the sediment material for the IC. We assume that the palaeogeographical and geomorphological characteristics of this periglacial landscape directly influenced the development of ecosystems in the region.

We suggest that the Bykovsky Peninsula IC is a distal type of deposits found as erosional remnants in the

Kharaulakh Ridge and its valleys. The Khorogor Valley was at least partially filled with IC-like deposits during the Late Pleistocene and was part of the gently inclined accumulation plain in the mountain foreland. The valley infill was eroded during the late Sartan between ca. 18 and 13.5 cal ky BP, when fluvial activity increased due to higher post-LGM summer temperatures and increased meltwater release from snowfields. The beginning disconnection of the foreland accumulation plain from sediment supply of the Kharaulakh Ridge was a result of fluvial erosion in the hinterland during the Late Glacial. The sedimentation gap on top of the Mamontovy Khayata outcrop section between ca. 12.5 and 9.4 cal ky BP can be attributed to thermokarst subsidence. The palaeo-environmental information derived from the new outcrops in the central and lower Khorogor Valley covers approximately the Bølling/Allerød and the Younger Dryas, and is useful for a better understanding of the Late Pleistocene/Holocene transition. Since that period, the slopes and plains in the Khorogor Valley are relatively stable, the fluvial activity remained high, and only minor accumulation took place. This indicates fundamental differences between Late Pleistocene and recent environmental variables in terms of snow accumulation, weathering, erosion and sediment transport in the Khorogor Valley.

With the beginning of the Holocene the former extensive accumulation plain was completely reshaped into a landscape dominated by extensive permafrost degradation. Thermokarst and thermo-erosion led to lake formation, ground subsidence, and the formation of distinct depressions. It is suggested that initial thermokarst preferentially started in previously existing negative relief forms like shallow streambeds or ground with cryolithological anomalies. Thermokarst had a major influence on the local hydrology, sediment deposition, and composition of ecosystems. Its maximum activity was during the Early Holocene Optimum, when the largest lakes existed. Afterwards, climate deterioration led to lake shrinking and talik refreezing. The modern outline of the peninsula was shaped by a combination of thermokarst, thermo-erosion, thermo-abrasion, coastal erosion, and marine inundation.

The general role of neotectonics in the regional landscape evolution is evident by e.g. the fault-influenced shape of the Khorogor Valley, although its influence on sedimentation patterns still has to be quantified.

Acknowledgements

References

Andreev, A.A., Schirrmeister, L., Siegert, C., Bobrov, A.A., Demske, D., Seiffert, M., Hubberten, H.-W., 2002. Paleoenvironmental changes in north-eastern Siberia during the Late Quaternary — evidence from pollen records of the Bykovsky Peninsula. Polarforschung 70, 13–25.

Bauch, H.A., Mueller-Lupp, T., Taldenkova, E., Spielhagen, R.F., Kassens, H., Grootes, P.M., Thiede, J., Heinemeier, J., Petryashov, V.V., 2001. Chronology of the Holocene transgression at the North Siberian margin. Global and Planetary Change 31, 125–139.

Berger, A., Loutre, M.F., 1991. Insolation values for the climate of the last 10 million years. Quaternary Science Reviews 10, 297–317.

Bobrov, A.A., Andreev, A.A, Schirrmeister, L., Siegert, C., 2004. Testate amoebae (Protozoa: *Testacealobosea* and *Testaceafilosea*) as bioindicators in the Late Quaternary deposits of the Bykovsky Peninsula, Laptev Sea, Russia. Palaeogeography, Palaeoclimatology, Palaeoecology 209, 165–181.

Dansgaard, W., Johnson, S.J., Clausen, A.B., Dahl-Jensen, D., Gundestrup, N.S., Hammer, C.U., Hvidberg, C.S., Steffensen, J.P., Sveinbjornsdottir, A.E., Jouzel, J., Bond, G., 1993. Evidence for general instability of past climate from a 250-kyr ice-core record. Nature 364, 218–220.

Drachev, S.S., Savostin, L.A., Groshev, V.G., Bruni, I.E., 1998. Structure and geology of the continental shelf of the Laptev Sea, Eastern Russian Arctic. Tectonophysics 298, 357–393.

Fairbanks, R.G., 1989. A 17,000-year glacio-eustatic sea level record: influence of glacial melting rates on the Younger Dryas event and deep-ocean circulation. Nature 342, 637–642.

Fedorov, A., Konstantinov, P., 2003. Observations of surface dynamics with thermokarst initiation, Yukechi site, Central Yakutia. Proceedings of the 8th International Permafrost Conference. Zurich, Switzerland, pp. 239–243.

Franke, D., Hinz, K., Oncken, O., 2001. The Laptev sea rift. Marine and Petroleum Geology 18, 1083–1127.

French, H.M., 1996. The Periglacial Environment, 2nd ed. Longman, Harlow.

Galabala, R.O., 1997. Pereletki and the initiation of glaciation in Siberia. Quaternary International 41–42, 27–32.

Gavrilov, A.V., Romanovskii, N.N., Romanovsky, V.E., Hubberten, H.-W., Tumskoy, V.E., 2003. Reconstruction of Ice Complex remnants on the Eastern Siberian Arctic shelf. Permafrost and Periglacial Processes 14, 187–198.

Goward, S.N., Masek, J.G., Williams, D.L., Irons, J.R., Thompson, R.J., 2001. The Landsat 7 mission: terrestrial research and applications for the 21st century. Remote Sensing of Environment 78, 3–12.

Gravis, G.F., 1969a. Sklonovye otlozheniya Yakutii (Slope Deposits of Yakutia). Nauka, Moscow. (in Russian).

Gravis, G.F., 1969b. Fossil slope deposits in the northern Arctic asymmetrical valleys. Biuletyn Peryglacjalny 20, 239–257.

Grigoriev, M.N., 1993. Kriomorfogenez ust'evoi oblast p. Leny (Cryomorphogenesis in the Lena Delta). Permafrost Institute Press, Yakutsk. (in Russian).

Grigoriev, M.N., Imaev, V.S., Kozmin, B.M., Kunitsky, V.V., Larionov, A.G., Mikulenko, K.I., Skrjabin, R.M., Timirsin, K.V., 1996. Geology, Seismicity and Cryogenic Processes in the Arctic Areas of Western Yakutia. Yakutian Scientific Centre SB RAS, Yakutsk. (in Russian).

Grinenko, O.V., Imaev, V.S., 1989. Cenozoic thrusts of the northern part of the Kharaulakh Ridge. Geologiya i Geofizika 5, 121–123 (in Russian).

Grinenko, O.V., Sergeenko, A.I., Belolyubskiy, I.N., 1998. Regional'naya stratigrafichskaya skhema paleogenovykh i neogenovykh otlozhenii Severo-Vostoka Rossii i obyasnitel'naya zapiska k nei [Regional stratigraphic chart for the Paleogene and Neogene deposits in North-Eastern Russia and the explanatory note]. Interdepartmental Stratigraphic Committee, Russian Academy of Science: Paleogen i neogen Severo-Vostoka Rossii [Paleogene and Neogene of Northeastern Russia, Part 2], pp. 5–35 (Yakutsk in Russian).

Grosse, G., Schirrmeister, L., Kunitsky, V.V., Dereviagyn, A.Y., 2003. Periglacial features around Tiksi. AWI Reports on Polar and Marine Research 466, 137–191.

Grosse, G., Schirrmeister, L., Kunitsky, V.V., Hubberten, H.-W., 2005. The use of CORONA images in remote sensing of periglacial geomorphology: an illustration from the NE Siberian coast. Permafrost and Periglacial Processes 16, 163–172.

Grosse, G., Schirrmeister, L., Malthus, T.J., 2006. Application of Landsat-7 satellite data and a DEM for the quantification of thermokarst-affected terrain types in the periglacial Lena–Anabar coastal lowland. Polar Research 25, 51–67.

Hubberten, H.-W., Andreev, A., Astakhov, V.I., Demidov, I., Dowdeswell, J.A., Henriksen, M., Hjort, C., Houmark-Nielsen, M., Jakobsson, M., Larsen, E., Lunkka, J.P., Lyså, A., Mangerud, J., Möller, P., Saarnisto, M., Schirrmeister, L., Sher, A.V., Siegert, C., Siegert, M.J., Svendsen, J.I., 2004. The periglacial climate and environment in northern Eurasia during the last glaciation (LGM). Quaternary Science Reviews 23, 1333–1357.

Imaev, V.S., Imaeva, L.P., Kozmin, B.M., 2000. Seismotektonika Yakutii [Seismo-tectonics of Yakutia]. GEOS, Moscow. (in Russian).

Katasonova, E.G., 1963. Rol' termokarsta v rasvitii dellei [The role of thermokarst in the development of delly]. In: Katasonov, E.M. (Ed.), Usloviya i osobennosti rasvitiya merslykh tolshch v Sibirii i na Severo-Vostoke [Conditions and special features of the formation of frozen horizons in Siberia and in Far-East]. Publishing House AN SSSR, Moscow, pp. 91–100 (in Russian).

Kholodov, A.L, Rivkina, E.M., Gilichinsky, D.A., Fyodorov-Davydov, D.G., Gubin, S.V., Sorokovikov, V.A., Ostroumov, V.E., Maksimovich, S.V., 2003. Estimation of the organic carbon input into Arctic ocean due to erosion of Laptev and East-Siberian seashore. Kriosfera Zemli 3, 3–12 (in Russian).

Kienast, F., Schirrmeister, L., Siegert, C., Tarasov, P., 2005. Palaeobotanical evidence for warm summers in the East Siberian Arctic during the last cold stage. Quaternary Research 63, 283–300.

Kind, N.V., 1975. Glaciations in the Verkhojansk Mountains and their place in the radiocarbon chronology of the Late Pleistocene Anthropogene. Biuletyn Peryglacjalny 24, 41–54.

Konishchev, V.N., Rozenbaum, G.E., Romanovsky, N.N., 1999. In: Melnikov, V.P. (Ed.), Russian–English Glossary of Geocryology and Related Scientific Fields. MSU Press, Moscow.

Kunitsky, V.V., 1989. Kriolitologiya nizo'ev Leny (Cryolithology of the Lower Lena). Permafrost Institute Press, Yakutsk. (in Russian).

Kunitsky, V.V., Schirrmeister, L., Grosse, G., Kienast, F., 2002. Snow patches in nival landscapes and their role for the Ice Complex formation in the Laptev Sea coastal lowlands. Polarforschung 70, 53–67.

Lewkowicz, A.G., 1981. A study of slopewash processes in the continuous permafrost zone, Western Canadian Arctic. Ph.D. Thesis, University of Ottawa, Canada.

Lewkowicz, A.G., Kokelj, S.V., 2002. Slope sediment yield in arid lowland continuous permafrost environments, Canadian Arctic Archipelago. Catena 46, 261–283.

Meyer, H., Dereviagin, A.Y., Siegert, C., Hubberten, H.-W., 2002a. Paleoclimate studies on Bykovsky Peninsula, North Siberia — Hydrogen and oxygen isotopes in ground ice. Polarforschung 70, 37–51.

Meyer, H., Dereviagin, A., Siegert, C., Schirrmeister, L., Hubberten, H.-W., 2002b. Palaeoclimate reconstruction on Big Lyakhovsky Island, North Siberia — hydrogen and oxygen isotopes in ice wedges. Permafrost and Periglacial Processes 13, 91–105.

Nagaoka, D., 1994. Properties of Ice Complex deposits in Eastern Siberia. Proceedings of the 2nd Symposium on the Joint Siberian Permafrost Studies between Japan and Russia in 1993. Tsukuba, Japan, pp. 14–18.

Nagaoka, D., Saijo, K., Fukuda, M., 1995. Sedimental environment of the Edoma in high Arctic eastern Siberia. Proceedings of the 3rd Symposium on the Joint Siberian Permafrost Studies between Japan and Russia in 1994. Hokkaido University Press, Sapporo, Japan, pp. 8–13.

Parfenov, L.M. (Ed.), 2001. Tektonika, geodinamika i metalogeniya territorii respubliki Sakha (Yakutiya) [Tectonics, Geodynamics, and Metallogeny of the Sakha Republic (Yakutia)]. Nauka Interperiodika, Moscow. (in Russian).

Rachold, V., Eicken, H., Gordeev, V.V., Grigoriev, M.N., Hubberten, H.-W., Lisitzin, A.P., Shevchenko, V.P., Schirrmeister, L., 2003. Modern terrigenous organic carbon input to the Arctic Ocean. In: Stein, R., Macdonald, R.W. (Eds.), Organic Carbon Cycle in the Arctic Ocean: Present and Past. Springer, Berlin, pp. 33–55.

Romanovskii, N.N., Hubberten, H.-W., Gavrilov, A.V., Tumskoy, V.E., Kholodov, A.L., 2004. Permafrost of the east Siberian Arctic shelf and coastal lowlands. Quaternary Science Reviews 23, 1359–1369.

Rutter, N.W., Rokosh, D., Evans, M.E., Little, E.C., Chlachula, J., Velichko, A., 2003. Correlation and interpretation of paleosols and loess across European Russia and Asia over the last interglacial–glacial cycle. Quaternary Research 60, 101–109.

Schirrmeister, L., Kunitsky, V., Grosse, G., Kuznetsova, T., Kuzmina, S., Bolshianov, D., 2001. Late Quaternary and recent environmental situation around the Olenyok Channel (western Lena Delta) and on Bykovsky Peninsula. AWI Reports on Polar and Marine Research 388, 85–135.

Schirrmeister, L., Siegert, C., Kuznetsova, T., Kuzmina, S., Andreev, A.A., Kienast, F., Meyer, H., Bobrov, A., 2002a. Paleoenvironmental and paleoclimatic records from permafrost deposits in the Arctic region of Northern Siberia. Quaternary International 89, 97–118.

Schirrmeister, L., Siegert, C., Kunitsky, V.V., Grootes, P.M., Erlenkeuser, H., 2002b. Late Quaternary ice-rich permafrost sequences as a paleoenvironmental archive for the Laptev Sea Region in northern Siberia. International Journal of Earth Sciences 91, 154–167.

Schirrmeister, L., Grosse, G., Schwamborn, G., Andreev, A.A., Meyer, H., Kunitsky, V.V., Kuznetsova, T.V., Dorozhkina, M.V., Pavlova, E.Y., Bobrov, A.A., Oezen, D., 2003. Late Quaternary History of the Accumulation Plain North of the Chekanovsky Ridge (Lena

Delta, Russia): a Multidisciplinary Approach. Polar Geography 27, 277–319.

Schwamborn, G., Rachold, V., Grigoriev, M.N., 2002. Late Quaternary sedimentation history of the Lena Delta. Quaternary International 89, 119–134.

Sergienko, A.I., Belolyubsky, I.N., Grinenko, O.V., 2004. Stratigraphic scheme of Quaternary deposits of the northern Verkhoyan (Eastern Yakutia). Otechestvennaya Geologiya 4, 88–92 (in Russian).

Sher, A., Parmuzin, I., Bartsov, A., 2000. Ice Complex on Bykovsky Peninsula. AWI Reports on Polar and Marine Research 354, 169–182.

Sher, A.V., Kuzmina, S.A., Kuznetsova, T.V., Sulerzhitsky, L.D., 2005. New insights into the Weichselian environment and climate of the East Siberian Arctic, derived from fossil insects, plants, and mammals. Quaternary Science Reviews 24, 533–569.

Siegert, C., Schirrmeister, L., Kunitsky, V.V., Meyer, H., Kuznetsova, T., Dereviagyn, A., Kuzmina, S., Tumskoy, V., Sher, A., 1999. Paleoclimate signals of ice-rich permafrost. AWI Reports on Polar and Marine Research 315, 145–259.

Siegert, C., Schirrmeister, L., Babiy, O., 2002. The sedimentological, mineralogical and geochemical composition of Late Pleistocene deposits from the Ice Complex on the Bykovsky Peninsula, Northern Siberia. Polarforschung 70, 3–11.

Slagoda, E.A., 1993. Genesis i mikrostroenie kriolitogennykh otlozhenii Bykovskogo polyostrova i ostrova Muoastakh [Genesis and microstructure of cryolithogenic deposits at the Bykovsky Peninsula and the Muostakh Island]. Ph.D. Thesis. Russian Academy of Science, Siberian Branch, Permafrost Institute Yakutsk. (in Russian).

Slagoda, E.A., 2004. Kriogennye otlozheniya Primorskoi ravniny morya Laptebykh: litologiya i mikromorfologiya [Cryolithogenic Deposits of the Laptev Sea Coastal Plain: Lithology and Micromorphology]. Publishing and Printing Centre "Express", Tyumen. (in Russian).

Slagoda, E.A., 2005. Cryogenic structure and genesis of Late Cenozoic watershed formations at the Primorsky mountain range adjacent to the Bykovsky Peninsula, Laptev Sea, Russia. 2nd European Conference on Permafrost, Potsdam, Germany, pp. 23–24.

Spielhagen, R.F., Erlenkeuser, H., Siegert, C., 2005. History of freshwater runoff across the Laptev Sea (Arctic) during the last deglaciation. Global and Planetary Change 48, 187–207.

Stratigrafiya SSSR (Stratigraphy of the USSR), 1982. Chetvertichnaya systema (Quaternary System, Volume 1). Nedra, Moscow. (in Russian).

Stratigrafiya SSSR (Stratigraphy of the USSR), 1984. Chetvertichnaya systema [Quaternary System, volume 2]. Nedra, Moscow. (in Russian).

Stromquist, L., 1985. Geomorphic impact of snowmelt on slope erosion and sediment production. Zeitschrift für Geomorphologie 29, 129–138.

Stuiver, M., Reimer, P.J., Bard, E., Beck, J.W., Burr, G.S., Hughen, K.A., Kromer, B., McCormac, G., van der Plicht, J., Spurk, M., 1998. INTCAL98 radiocarbon age calibration, 24000-0 cal BP. Radiocarbon 40, 1041–1083.

Svendsen, J.I., Alexanderson, H., Astakhov, V.I., Demidov, I., Dowdeswell, J.A., Funder, S., Gataullin, V., Henriksen, M., Hjort, Ch., Houmark-Nielsen, M., Hubberten, H.-W., Ingólfsson, Ó., Jakobsson, M., Kjær, K.H., Larsen, E., Lokrantz, H., Lunkka, J.P., Lyså, A., Mangerud, J., Matiouchkov, A., Murray, A., Möller, P., Niessen, F., Nikolskaya, O., Polyak, L., Saarnisto, M., Siegert, C., Siegert, M.J., Spielhagen, R.F., Stein, R., 2004. Late Quaternary ice sheet history of northern Eurasia. Quaternary Science Reviews 23, 1229–1271.

Tomirdiaro, S.V., Arslanov, K.A., Chernen'kiy, B.I., Tertychnaya, T.V., Prokhorova, T.N., 1984. Novie dannye o formirovanii lyessovo-ledovykh tolcsh Severnoi Yakutii i usloviya obitaniya mamontovoy faunny v Arktike v pozdnem pleistotsene (New data on formation of loess-ice sequences in northern Yakutia and ecological conditions of mammoth fauna in the Arctic during the Late Pleistocene). Doklady AN SSSR 278 (6), 1446–1449 (in Russian).

Treshnikov, A.F., 1985. Atlas Arktiki (Atlas of the Arctic). National Commission of Hydro-Meteorology and Environmental Protection, Major Department of Geodesy and Cartography. USSR, Moscow. (in Russian).

Ursov, A.S., Prokop'ev, B.S., Slastenov, Yu.L., 1999. Geologicheskaya karta Yakutii, 1:500,000, Zapato-Verkhoyanskii Blok [Geological Map of Yakutia, 1: 500,000, West Verkhoyansky Block]. National Yakutian Comittee of Geology and Resources, Yakutsk. (in Russian).

Velichko, A.A. (Ed.), 1999. Izmenenie klimata i landshaftov za poslednie 65 millionov let. (Climate and Environment Changes during the Last 65 Million Years). GEOS, Moscow. (in Russian).

Velichko, A.A., Catto, N., Drenova, A.N., Klimanov, V.A., Kremenetski, K.V., Nechaev, V.P., 2002. Climate changes in East Europe and Siberia at the Late Glacial–Holocene transition. Quaternary International 91, 75–99.

Wilkinson, T.J., Bunting, B.T., 1975. Overland transport of sediment by rill water in a periglacial environment in the Canadian High Arctic. Geografiska Annaler 57A, 105–116.

Yershov, E.D., 1998. General Geocryology — Studies in Polar Research. Cambridge University Press, Cambridge.